AMERICAN SOCIETY FOR MICROBIOLOGY | Journal of Virology®

CELLULAR RESPONSE TO INFECTION

HOIL1 Is Essential for the Induction of Type I and III Interferons by MDA5 and Regulates Persistent Murine Norovirus Infection

Donna A. MacDuff,[a,b]* Megan T. Baldridge,[a,c]* Arwa M. Qaqish,[b] Timothy J. Nice,[a]* Azad D. Darbandi,[b] Victoria L. Hartley,[b] Stefan T. Peterson,[c] Jonathan J. Miner,[c] Kazuhiro Iwai,[d] Herbert W. Virgin[a]

[a]Department of Pathology and Immunology, Washington University School of Medicine, St. Louis, Missouri, USA

[b]Department of Microbiology and Immunology, University of Illinois at Chicago, Chicago, Illinois, USA

[c]Department of Medicine, Washington University School of Medicine, St. Louis, Missouri, USA

[d]Department of Molecular and Cellular Physiology, Graduate School of Medicine, Kyoto University, Kyoto, Japan

ABSTRACT The linear ubiquitin chain assembly complex (LUBAC), composed of heme-oxidized IRP2 ubiquitin ligase 1 (HOIL1), HOIL1-interacting protein (HOIP), and SHANK-associated RH domain-interacting protein (SHARPIN), is a crucial regulator of multiple immune signaling pathways. In humans, HOIL1 or HOIP deficiency is associated with an immune disorder involving autoinflammation, immunodeficiency, and inflammatory bowel disease (IBD)-like symptoms. During viral infection, LUBAC is reported to inhibit the induction of interferon (IFN) by the cytosolic RNA sensor retinoic acid-inducible gene I (RIG-I). Surprisingly, we found that HOIL1 is essential for the induction of both type I and type III IFNs, as well as the phosphorylation of IFN regulatory factor 3 (IRF3), during murine norovirus (MNoV) infection in cultured dendritic cells. The RIG-I-like receptor, melanoma differentiation-associated protein 5 (MDA5), is also required for IFN induction and IRF3 phosphorylation during MNoV infection. Furthermore, HOIL1 and MDA5 were required for IFN induction after Theiler's murine encephalomyelitis virus infection and poly(I·C) transfection, but not Sendai virus or vesicular stomatitis virus infection, indicating that HOIL1 and LUBAC are required selectively for MDA5 signaling. Moreover, *Hoil1*$^{-/-}$ mice exhibited defective control of acute and persistent murine norovirus infection and defective regulation of MNoV persistence by the microbiome as also observed previously for mice deficient in interferon lambda (IFN-λ) receptor, signal transducer and activator of transcription factor 1 (STAT1), and IRF3. These data indicate that LUBAC plays a critical role in IFN induction to control RNA viruses sensed by MDA5.

IMPORTANCE Human noroviruses are a leading cause of gastroenteritis throughout the world but are challenging to study *in vivo* and *in vitro*. Murine norovirus (MNoV) provides a tractable genetic and small-animal model to study norovirus biology and immune responses. Interferons are critical mediators of antiviral immunity, but excessive expression can dysregulate the immune system. IFN-λ plays an important role at mucosal surfaces, including the gastrointestinal tract, and both IFN-λ and commensal enteric bacteria are important modulators of persistent MNoV infection. LUBAC, of which HOIL1 is a component, is reported to inhibit type I IFN induction after RIG-I stimulation. We show, in contrast, that HOIL1 is critical for type I and III IFN induction during infection with MNoV, a virus that preferentially activates MDA5. Moreover, HOIL1 regulates MNoV infection *in vivo*. These data reveal distinct functions for LUBAC in these closely related signaling pathways and in modulation of IFN expression.

Received 8 August 2018 **Accepted** 6 September 2018

Accepted manuscript posted online 12 September 2018

Citation MacDuff DA, Baldridge MT, Qaqish AM, Nice TJ, Darbandi AD, Hartley VL, Peterson ST, Miner JJ, Iwai K, Virgin HW. 2018. HOIL1 is essential for the induction of type I and III interferons by MDA5 and regulates persistent murine norovirus infection. J Virol 92:e01368-18. https://doi.org/10.1128/JVI.01368-18.

Editor Julie K. Pfeiffer, University of Texas Southwestern Medical Center

Address correspondence to Donna A. MacDuff, dmacduff@uic.edu, or Herbert W. Virgin, virgin@wustl.edu.

* Present address: Donna A. MacDuff, Department of Microbiology and Immunology, University of Illinois at Chicago, Chicago, Illinois, USA; Megan T. Baldridge, Department of Medicine, Washington University School of Medicine, St. Louis, Missouri, USA; Timothy J. Nice, Department of Molecular Microbiology and Immunology, Oregon Health and Science University, Portland, Oregon, USA.

D.A.M. and M.T.B. contributed equally to this work.

KEYWORDS HOIL1, LUBAC, MDA5, interferons, norovirus, ubiquitination

Infection with human norovirus (HNoV) is the leading global cause of acute gastroenteritis and an important cause of hospitalization and death, particularly in children, elderly, and immunocompromised individuals (1, 2). However, studies of HNoV biology and immunity have been hindered by the lack of a robust animal model or cell culture system (3). Murine norovirus (MNoV) infects laboratory mice *in vivo* and can be grown in murine dendritic cells, macrophages, and B cells *in vitro*, and thereby provides a powerful model to study both viral and host factors that contribute to the biology, immunity, and pathogenesis of norovirus (4). MNoV has also proven to be a useful model to interrogate interactions between a mucosal virus and the commensal bacterial microbiome, with recent reports highlighting a significant role for bacteria in facilitating viral infection (5, 6), at least in part through the modulation of interferon lambda (IFN-λ) signaling (5, 7).

IFNs play a critical role in antiviral immunity through the induction of hundreds of interferon-stimulated genes (ISGs), many of which possess direct antiviral function, and through the activation of adaptive immunity (8). Type I IFNs signal through the interferon alpha receptor (IFNAR) to activate the Janus kinase and signal transducer and activator of transcription (JAK-STAT) pathway to induce ISG transcription (9). Type III IFN, also known as interferon lambda (IFN-λ) or interleukin 28 (IL-28)/IL-29, binds to an IL-28 receptor alpha (IL-28Rα)/IL-10Rβ heterodimeric receptor (IFNLR) to activate the JAK-STAT pathway and plays an important role in antiviral immunity at mucosal surfaces, including the lung and gastrointestinal tract (10–12). Investigation of host-virus interactions has uncovered critical roles for both type I and type III IFNs in the regulation of acute and persistent strains of MNoV (5, 7, 13, 14). Indeed, administration of a single dose of IFN-λ is sufficient to induce clearance of MNoV from persistently infected mice in an IFNLR-dependent manner that does not require the participation of the adaptive immune system (7, 15).

IFN can be induced in virally infected cells through the activation of several different pattern recognition receptors (8). Sensing of viral RNA replication products in the cytoplasm by retinoic acid-inducible gene I (RIG-I/DDX58) or melanoma differentiation-associated protein 5 (MDA5/IFIH1) leads to the aggregation of the adaptor mitochondrial antiviral signaling protein (MAVS; also known as VISA, IPS-1, and CARDIF), and the subsequent recruitment and activation of kinases TANK-binding kinase 1 (TBK1) and inhibitor of kappa B kinase epsilon (IKKε). TBK1 and IKKε phosphorylate and activate transcription factors such as interferon regulatory factor 3 (IRF3) and IRF7 (16). Detection of viral RNA in endosomes by Toll-like receptor 3 (TLR3), TLR7, or TLR8, or viral proteins by TLR2 or TLR4, also leads IFN induction via the adaptors TIR domain-containing adaptor-inducing interferon beta (TRIF) and myeloid differentiation factor 88 (MyD88), and the transcription factors interferon regulatory factor 3 (IRF3), IRF7, and NF-κB (17). Induction of interferon beta (IFN-β) by MNoV strain CW3 is largely dependent on MDA5, with only a minor role observed for TLR3 *in vivo* (18). IRF3, but not IRF7, has been implicated in regulation of the interaction between MNoV and bacteria (5), though both factors may control MNoV replication *in vivo* (19).

In addition to protein phosphorylation, polyubiquitination also plays a central role in immune signaling pathways (20, 21). The linear ubiquitin chain assembly complex (LUBAC), composed of heme-oxidized IRP2 ubiquitin ligase 1 (HOIL1; also known as Rbck1), HOIL1-interacting protein (HOIP; also known as Rnf31), and SHANK-associated RH domain-interacting protein (SHARPIN), is an important modulator of innate immunity and inflammation (21–31). LUBAC is the only known generator of linear (methionine-1-linked) polyubiquitin chains (32–35), and it has been increasingly tied to regulation of diverse signaling pathways involved in immune responses, cell death, and cancer (36, 37).

In humans, HOIL1 deficiency is associated with a complex disorder, including an immunodeficiency associated with increased susceptibility to pyogenic bacterial infec-

tions, an autoinflammatory syndrome, inflammatory bowel disease (IBD)-like symptoms, myopathy and cardiomyopathy associated with amylopectinosis (26), or amylopectinosis and myopathy alone (38, 39). HOIP deficiency results in a similar immune disorder (24), whereas SHARPIN-deficient patients have not been described thus far.

In mice, HOIP deficiency results in embryonic lethality (40), whereas SHARPIN-deficient mice are viable but suffer from a chronic proliferative dermatitis (41–43). These observations suggest that, while the three proteins function together within the LUBAC, cell type-specific or LUBAC-independent functions may exist for the individual proteins *in vivo*. Two recent studies have shown that mice fully deficient for HOIL1 also die during embryogenesis (44, 45). However, expression of the N-terminal half of HOIL1 at approximately 10% of wild-type levels is sufficient to confer viability, and these mice (*Hoil1*$^{-/-}$ mice hereafter) appear to be phenotypically normal when housed under specific-pathogen-free conditions, except for amylopectinosis in the cardiac tissue of older animals (23, 34, 45). In response to infection, we found previously that *Hoil1*$^{-/-}$ mice exhibit increased mortality upon infection with some bacterial pathogens, but enhanced control of others (23). With regard to viral pathogens, reactivation of murine gammaherpesvirus 68 from latency is suppressed in *Hoil1*$^{-/-}$ mice, correlating with elevated type II IFN and proinflammatory cytokine production (23). Others have shown that SHARPIN-deficient mice display increased susceptibility to influenza A virus infection due to impaired TLR3-mediated antiviral response and enhanced TLR3-induced cell death (43).

At the cellular level, LUBAC is essential for efficient NF-κB activation downstream of many important immune receptors, including TLRs, tumor necrosis factor receptor 1 (TNFR1), and interleukin 1 receptor 1 (IL1R1) (22, 27, 46, 47), and for activation of the NLRP3 inflammasome (48). In contrast, LUBAC has been shown to inhibit RIG-I signaling and type I IFN induction during Sendai virus (SeV) and vesicular stomatitis virus (VSV) infection in cultured cells through several independent mechanisms (49–53). Together, these studies indicate that, while required for proinflammatory cytokine production, LUBAC inhibits IFN induction by the RIG-I pathway during infection with negative-sense single-stranded RNA [(−)ssRNA] viruses.

Here, we show that HOIL1 is essential for the induction of type I and III IFNs after infection of cells with positive-sense ssRNA [(+)ssRNA] viruses, MNoV and Theiler's murine encephalomyelitis virus (TMEV), two viruses that are primarily sensed by MDA5 (18, 54). Defects in IFN induction were associated with impaired IRF3 and TBK1 phosphorylation during MNoV infection, with comparable levels in HOIL1- and MDA5-deficient cells, indicating that HOIL1 and the LUBAC are required for MDA5-dependent IFN induction. In contrast, neither HOIL1 nor MDA5 was required for IFN induction after infection with (−)ssRNA viruses, SeV and VSV. Furthermore, we show that HOIL1 regulates acute and persistent norovirus infection, as well as the dependence of MNoV CR6 on the commensal microbiota to establish persistent infection in mice *in vivo*, similar to IFNLR, IRF3, and STAT1 (5). These findings identify a novel role for HOIL1 in the MDA5-dependent IFN response to an RNA virus.

RESULTS

HOIL1 regulates persistent MNoV infection and dependence upon the commensal enteric microbiota. Since HOIL1 plays important roles downstream of many immune signaling pathways, including TLRs, Nod-like receptors (NLRs), and several cytokine receptors, we considered the possibility that HOIL1 may regulate the complex interaction between the host, commensal bacteria, and MNoV persistence. To test this hypothesis, *Hoil1*$^{-/-}$ and control mice received a broad-spectrum cocktail of antibiotics for two weeks prior to inoculation with MNoV CR6. While antibiotic pretreatment prevented MNoV persistence in control mice as expected, antibiotic-treated *Hoil1*$^{-/-}$ mice were robustly infected as measured by viral genome copies in both stool and tissue samples 14 days postinfection (dpi) (Fig. 1A and B). Notably, even in the absence of antibiotic pretreatment, *Hoil1*$^{-/-}$ mice exhibited elevated persistent viral loads in stool and intestinal tissue samples. *Hoil1*-deficient mice thus phenocopy *Ifnlr1*-, *Stat1*-, and *Irf3*-deficient mice for effects on viral

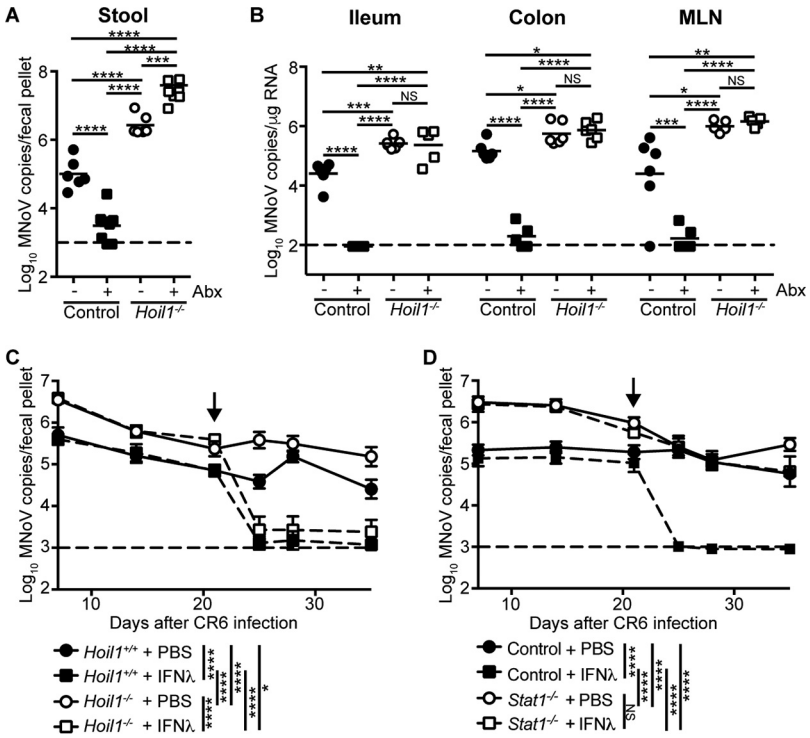

FIG 1 HOIL1 regulates the dependence of MNoV infection on commensal bacteria, but not its sensitivity to IFN-λ treatment. (A and B) MNoV genome copies detected in stool 7 days (A) or detected in ileum, colon, and mesenteric lymph nodes (MLN) 14 days (B) after MNoV CR6 inoculation of wild-type and *Hoil1*$^{-/-}$ mice pretreated with antibiotics (Abx) (vancomycin, neomycin, ampicillin, and metronidazole) for two weeks. Each symbol represents the value for an individual mouse. There were five to nine mice per group. Data are from three independent experiments. Results were analyzed by one-way analysis of variance (ANOVA) with Tukey's multiple-comparison test. (C and D) MNoV genome copies in stools of wild-type and *Hoil1*$^{-/-}$ (C) or *Stat1*$^{-/-}$ (D) mice persistently infected with MNoV CR6 and treated by intraperitoneal injection of 25 μg of IFN-λ or PBS 21 days postinfection (vertical black arrows). Results were analyzed by two-way ANOVA with Tukey's multiple-comparison test. There were 7 to 14 mice per group, and data are from two to three independent experiments. The limit of detection is indicated by dashed lines in the graphs. Values that are significantly different by ANOVA are indicated by bars and asterisks as follows: *, $P < 0.05$; **, $P < 0.01$; ***, $P < 0.001$; ****, $P < 0.0001$. Values that are not significantly different ($P > 0.05$) by ANOVA are indicated (NS).

replication and a role in microbiome control of persistent norovirus infection (5), suggesting that HOIL1 functions in the IFN-λ pathway.

To determine whether HOIL1 is required for IFN-λ signaling and antiviral effects, persistently infected control and *Hoil1*$^{-/-}$ mice were treated with recombinant IFN-λ at a dose sufficient to induce clearance of persistent MNoV CR6 infection in wild-type mice (7) (Fig. 1C). Despite higher viral loads in *Hoil1*$^{-/-}$ mice, IFN-λ induced MNoV clearance in these mice similar to control mice (Fig. 1C). In contrast, IFN-λ treatment had no effect on viral levels in mice deficient for STAT1, a transcription factor essential for IFN-λ signaling (Fig. 1D). These data indicate that HOIL1 is not required for antiviral signaling downstream of IFNLR *in vivo*.

HOIL1 is required for induction of type I and III IFNs in response to MNoV infection *in vitro*. Since HOIL1 is not required for the antiviral effects of IFN-λ, but IFN-λ and HOIL1 regulate MNoV infection *in vivo*, we asked whether HOIL1 is necessary for the induction of IFN-λ in response to MNoV infection. Dendritic cells are considered to be an important site for MNoV replication *in vivo* and support viral replication *in vitro* (55–57). Therefore, control and *Hoil1*$^{-/-}$ bone marrow-derived dendritic cells (BMDCs) were infected with MNoV CR6 *in vitro*, and expression of transcripts encoding IFN-λ and IFN-β were measured by quantitative reverse transcription-PCR (qRT-PCR) over 12 h. While expression of both type I and III IFNs was substantially upregulated in control cells, IFN-λ-encoding transcripts were not detected, and IFN-β-encoding transcripts

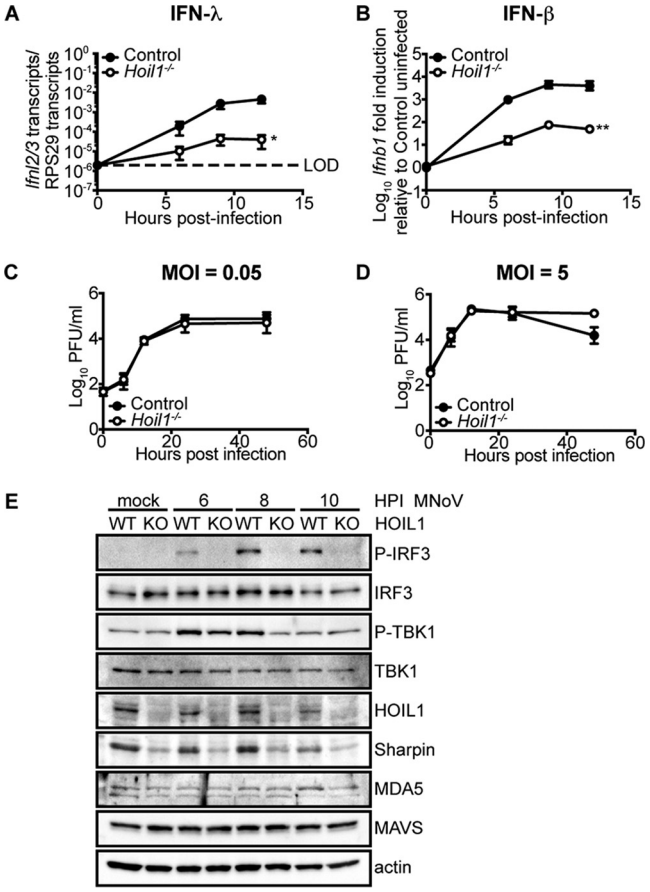

FIG 2 HOIL1 is required for induction of IFN-λ and IFN-β in BMDCs in response to MNoV infection. (A and B) *Ifnl2/3* (A) and *Ifnb1* (B) transcript expression in control and *Hoil1*$^{-/-}$ BMDCs after infection with MNoV CR6 at an MOI of 5. Data are from six independent experiments performed in duplicate. Results were analyzed by two-way ANOVA. The limit of detection (LOD) is indicated by the dashed line. Values are means ± standard errors of the means (SEM) (error bars). Values that are significantly different from the control value are indicated by asterisks as follows: *, $P < 0.05$; **, $P < 0.01$. (C and D) Growth of MNoV CR6 virus in *Hoil1*$^{-/-}$ and control BMDCs infected at a low (C) or high (D) MOI. Values are not significantly different as determined by paired *t* test. (E) Protein expression and phosphorylation in *Hoil1*$^{+/+}$ (wild-type [WT]) and *Hoil1*$^{-/-}$ (knockout [KO]) BMDCs at 6, 8, and 10 h postinfection (HPI) with MNoV CR6 and in mock-infected cells, analyzed by immunoblotting. Images are representative of three independent experiments. P-IRF3, phospho-IRF3.

were approximately 100-fold lower in *Hoil1*$^{-/-}$ BMDCs (Fig. 2A and B). This defect in IFN mRNA induction was not due to a requirement for HOIL1 for MNoV replication in these cells (Fig. 2C and D). These results were consistent with elevated levels of MNoV CR6 in *Hoil1*$^{-/-}$ mice *in vivo* and suggested a mechanism of viral control wherein HOIL1 is critical for viral sensing and the initiation of the innate antiviral response to infection.

HOIL1 is required for IRF3 phosphorylation after MNoV infection. The IRF3 transcription factor plays an important role in the induction of IFNs during viral infection and regulates persistent MNoV infection *in vivo* (5). Activation of IRF3 requires phosphorylation by the TBK1 and/or IKKε kinase, which induces IRF3 dimerization and translocation to the nucleus where it can initiate transcription (58). To determine whether HOIL1 was required for phosphorylation of IRF3, HOIL1−sufficient or -deficient BMDCs were collected 6, 8, and 10 h postinfection (hpi) with MNoV CR6, and IRF3 phosphorylation was assessed by Western blot analysis (Fig. 2E). While phosphorylated IRF3 is observed in control BMDCs at 6, 8, and 10 hpi, phosphorylated IRF3 was not detected in *Hoil1*$^{-/-}$ BMDCs, indicating that HOIL1 is necessary for phosphorylation of IRF3 after MNoV infection. We also assessed phosphorylation and activation of the kinases for IRF3, TBK1, and IKKε. We were unable to detect phosphorylation of IKKε by

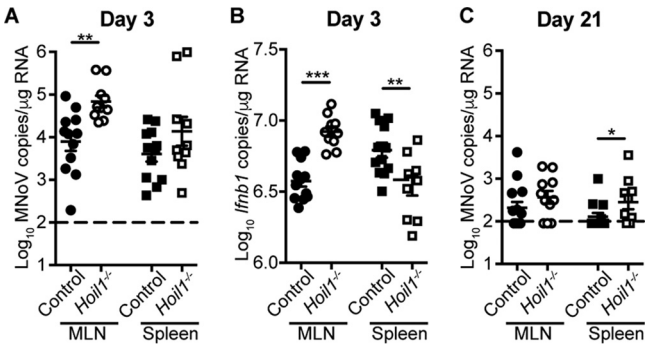

FIG 3 HOIL1 controls acute MNoV infection *in vivo*. (A and B) MNoV genome (A) and *Ifnb1* mRNA (B) copies detected in the mesenteric lymph nodes (MLN) and spleens of control and *Hoil1*$^{-/-}$ mice 3 days postinfection (dpi) with MNoV strain CW3. Each symbol represents the value for an individual mouse. Data were analyzed by unpaired *t* test with Welch's correction. There were 10 to 12 mice in each group. Data are from two independent experiments. (C) MNoV genome copies detected in MLN and spleens of control and *Hoil1*$^{-/-}$ mice 21 dpi with strain CW3. Each symbol represents the value for an individual mouse. Data were analyzed by Mann-Whitney test. There were 10 to 14 mice per group, from two independent experiments. The dashed line indicates the limit of detection for MNoV genome copies. Values that are significantly different are indicated by bars and asterisks as follows: *, $P < 0.05$; **, $P < 0.01$; ***, $P < 0.001$.

Western blot analysis at any time point analyzed (data not shown). Low levels of phosphorylated TBK1 were detected in mock-infected BMDCs (Fig. 2E). By 6 hpi, TBK1 was robustly phosphorylated in control cells but to a lesser extent in *Hoil1*$^{-/-}$ BMDCs. Phosphorylation of TBK1 was diminished at 8 hpi in the *Hoil1*$^{-/-}$ cells and returned to levels similar to those in mock-infected cells by 10 hpi. These data indicate that HOIL1 is required for the full phosphorylation and activation of TBK1, which likely contributes to the absence of phosphorylated IRF3 in infected cells. Total levels of IRF3, TBK1, MAVS, and MDA5 proteins were not affected by HOIL1 deficiency or MNoV infection. However, expression of the LUBAC component SHARPIN was reduced in *Hoil1*$^{-/-}$ cells as reported by others (Fig. 2E) (26, 27, 30, 31, 34). Together, these data show that HOIL1 is an important regulator of IFN induction via the TBK1-IRF3 pathway in response to MNoV infection of cultured dendritic cells.

HOIL1 regulates acute MNoV infection and IFN induction *in vivo*. While type III IFN is critical for control of persistent MNoV infection, type I IFN plays an important role in regulating acute, systemic infection (14, 19). To determine whether HOIL1 also restricts acute MNoV infection, control and *Hoil1*$^{-/-}$ mice were infected with acute MNoV strain CW3 (59). *Hoil1*$^{-/-}$ mice exhibited higher viral loads in the mesenteric lymph nodes (MLN) 3 dpi, indicating that HOIL1 controls initial acute MNoV infection or replication in this tissue. The increased viral loads in the MLN correlated with elevated levels of IFN-β mRNA (Fig. 3A and B). In the spleen, however, the numbers of MNoV genome copies were comparable in *Hoil1*$^{-/-}$ and control mice 3 dpi, but IFN-β levels were approximately twofold lower, indicating impaired IFN-β induction in *Hoil1*$^{-/-}$ mice in this tissue (Fig. 3A and B). This relatively small change in IFN-β induction observed in the spleen may reflect a difference in the kinetics of infection in *Hoil1*$^{-/-}$ mice, or it may be due to the involvement of multiple cell types and immune pathways by 3 dpi *in vivo*. Consistent with a reduced IFN response, viral loads were elevated in the spleens of *Hoil1*$^{-/-}$ mice 21 dpi, indicating delayed clearance of the virus from this tissue (Fig. 3C). These data indicate that HOIL1 also limits acute replication and enhances systemic clearance of the CW3 strain of MNoV and contributes to IFN induction *in vivo*.

Independent disruption of HOIL1 also impairs IFN induction during MNoV infection. Our data demonstrating defective IFN induction in HOIL1-deficient cells were inconsistent with other published studies, which emphasized a role for HOIL1 and LUBAC in suppressing IFN induction during RNA virus infection (49, 51–53). In addition, two recent studies reported that complete HOIL1 deficiency is embryonic lethal in mice (44, 45), similar

to HOIP deficiency (40). Consistent with those reports, we recently acquired *Hoil1* (*Rbck1*) "knockout first" mice with conditional potential (Rbck1$^{tm1a(EUCOMM)Hmgu}$) and observed that heterozygous matings of these mice failed to generate homozygous knockout pups (data not shown). These observations suggested that the *Hoil1*$^{-/-}$ mice used in the present study express a truncated protein and are hypomorphic. Fujita et al. showed that mouse embryonic fibroblasts (MEFs) derived from these mice express a small amount of a 29-kDa N-terminal fragment of HOIL1 that contains the ubiquitin-like (UBL) and NZF ubiquitin binding domains but lacks the RING-IBR-RING domains (45). We reported previously that HOIL1 mRNA levels are reduced approximately 10-fold in our *Hoil1*$^{-/-}$ mice (23), and here we found that full-length HOIL1 protein was not detected and SHARPIN protein levels were reduced by Western blot analysis (Fig. 2E), indicating that these mice are severely HOIL1 deficient. However, to confirm that our observed phenotypes were indeed due to HOIL1 deficiency, we generated an independent *Hoil1* knockout (KO) cell line using CRISPR/Cas9 technology in estrogen receptor (ER)-regulated HoxB8-immortalized precursor cells, which can be subsequently differentiated into dendritic cells (DCs) (60). First, we validated the ER-HoxB8 precursor cells and DCs for these studies by generating ER-HoxB8 precursor cell lines from *Hoil1*$^{+/+}$ and *Hoil1*$^{-/-}$ mice. After 7 days of differentiation into DCs in granulocyte-macrophage colony-stimulating factor (GM-CSF)-containing medium and infection with MNoV, induction of IFN-β mRNA was comparable to that observed in primary BMDCs from *Hoil1*$^{+/+}$ and *Hoil1*$^{-/-}$ mice (Fig. 4A and 2B). CRISPR/Cas9 targeting to *Hoil1* exon 6 induced a single nucleotide deletion on one allele and a single nucleotide insertion on the second allele (Fig. 4B), resulting in a D231fs (frameshift) mutation for both alleles. *Hoil1* mRNA was reduced by 75% in *Hoil1* KO ER-HoxB8 cells compared to controls (cells transduced with an empty vector single guide RNA [sgRNA], "Vector" herein) (Fig. 4C). While full-length protein was not detected by Western blot analysis, truncated protein products were visible, indicating that these cells are not fully HOIL1 deficient (Fig. 4D). However, SHARPIN protein levels were reduced, implying destabilization of the LUBAC in these cells as reported for deletion of individual components of the LUBAC (26, 27, 30, 31, 34) and observed for *Hoil1*$^{-/-}$ BMDCs (Fig. 4D and 2E).

After differentiation to DCs, 99.9% of the cells were CD11b^{+}, and approximately 50% were CD11c^{+} (data not shown), indicating that the cells were heterogeneous and displayed macrophage-like, as well as dendritic cell-like, characteristics. MNoV CR6 replicated robustly in both Vector and *Hoil1* KO ER-HoxB8 DCs and to similar titers as in BMDCs (Fig. 4E and Fig. 2C and D). Consistent with our findings from primary BMDCs described above, induction of IFN-λ and IFN-β mRNA was reduced approximately 10-fold in *Hoil1* KO ER-HoxB8 DCs compared to Vector DCs (Fig. 4F and G). However, we noted that IFN-λ mRNA levels in Vector ER-HoxB8 DCs were considerably lower than in control BMDCs, possibly due to the heterogeneity of the ER-HoxB8 DCs, and that these cells are likely not important producers of IFN-λ. We were unable to detect secreted IFN-λ protein in culture supernatants from either cell type by an enzyme-linked immunosorbent assay (ELISA) (data not shown). Additionally, IFN-β transcript levels were reduced by only 10-fold in *Hoil1* KO ER-HoxB8 DCs after MNoV infection (Fig. 4F). However, secreted IFN-β was detected in Vector, but not *Hoil1* KO, culture supernatants 12 and 24 hpi (Fig. 4H). Furthermore, phosphorylation of IRF3 and TBK1 was impaired in *Hoil1* KO ER-HoxB8 DCs (Fig. 4I). Together, these data corroborate that HOIL1 is important for efficient TBK1 and IRF3 phosphorylation and IFN induction during MNoV infection in cultured dendritic cells.

The MDA5-MAVS-IRF3/7 pathway regulates induction of IFNs by MNoV. Multiple pattern recognition receptor (PRR) pathways and mediators have been implicated in the activation of IRF3 and the induction of IFN-λ and IFN-β in response to viral pathogens (61, 62). The cytosolic double-stranded RNA (dsRNA) sensor MDA5 (IFIH1) plays an important role in the response to an acute strain of MNoV, CW3, *in vitro* and *in vivo*, whereas only a very minor role has been observed for TLR3 *in vivo* (18). To assess the roles of different pattern recognition receptor signaling pathways, we studied the induction of IFNs by MNoV in BMDCs from mice deficient in genes in the TLR- and

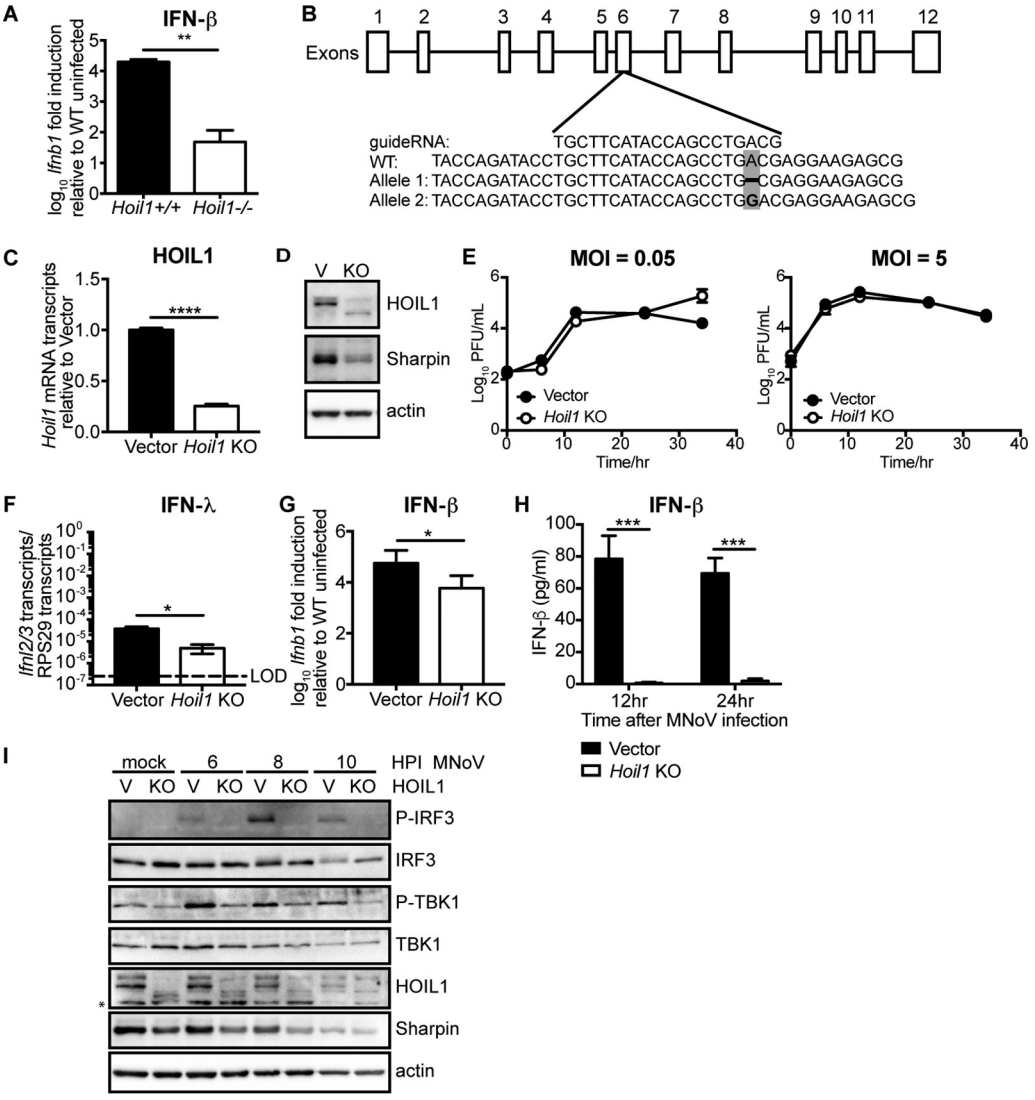

FIG 4 Independent disruption of *Hoil1* in BMDCs abrogates IFN induction during MNoV infection. (A) *Ifnb1* mRNA induction in ER-HoxB8 DCs derived from *Hoil1*$^{+/+}$ and *Hoil1*$^{-/-}$ mice 10 hpi with MNoV CR6 (MOI of 5). Data are from three independent experiments performed in duplicate. Data were analyzed by *t* test. (B) Schematic of the *Hoil1* gene to illustrate the position of the guide RNA targeted to exon 6, and the single nucleotide deletion and insertion in allele 1 and allele 2, respectively, of the *Hoil1* KO HoxB8 cell line (not to scale). (C) *Hoil1* mRNA expression in ER-HoxB8 DCs with *Hoil1* disrupted by CRISPR/Cas9 (*Hoil1* KO) or in cells transduced with an empty lentivirus (Vector). Data are from three independent experiments. Data were analyzed by *t* test. (D) Immunoblot analysis of HOIL1 and Sharpin protein expression in Vector (V) and *Hoil1* knockout (KO) ER-HoxB8 DCs. (E) Growth of MNoV CR6 virus in *Hoil1* KO and Vector control ER-HoxB8 DCs infected at a low (left panel) or high (right panel) MOI. Data are from three independent experiments performed in triplicate. Values are not significantly different as determined by paired *t* test. (F and G) *Ifnl2/3* (F) and *Ifnb1* (G) mRNA induction in *Hoil1* KO and Vector control ER-HoxB8 DCs 10 hpi with CR6 (MOI of 5). Data are from four independent experiments performed in duplicate. Data were analyzed by *t* test. The dashed line in panel F shows the limit of detection (LOD). (H) IFN-β protein levels in Vector and *Hoil1* KO cell culture supernatants 12 and 24 hpi with MNoV CR6 (MOI of 5) as measured by ELISA. (I) Protein expression and phosphorylation in *Hoil1* KO or Vector control ER-HoxB8 DCs at 6, 8, and 10 hpi with MNoV CR6 and in mock-infected cells, analyzed by immunoblotting. The position of a nonspecific band is indicated by an asterisk. Images are representative of three independent experiments. Data shown in panels A, C, E, F, G, and H are means plus SEM (or means ± SEM for panel F). Values that are significantly different are indicated by bars and asterisks as follows: *, $P < 0.05$; **, $P < 0.01$; ***, $P < 0.001$; ****, $P < 0.0001$.

MAVS-dependent pathways. *Mavs*$^{-/-}$ BMDCs showed a profound defect in IFN induction, similar to *Hoil1*$^{-/-}$ BMDCs, implicating RIG-I or MDA5 as the critical sensor of viral RNA (Fig. 5A and B). *Irf3*$^{-/-}$ and *Irf7*$^{-/-}$ BMDCs also showed substantial deficits in IFN-λ mRNA induction (Fig. 5A) and partial reductions in IFN-β mRNA induction (Fig. 5B, left panel), suggesting an important, and possibly combinatorial, role for these two transcrip-

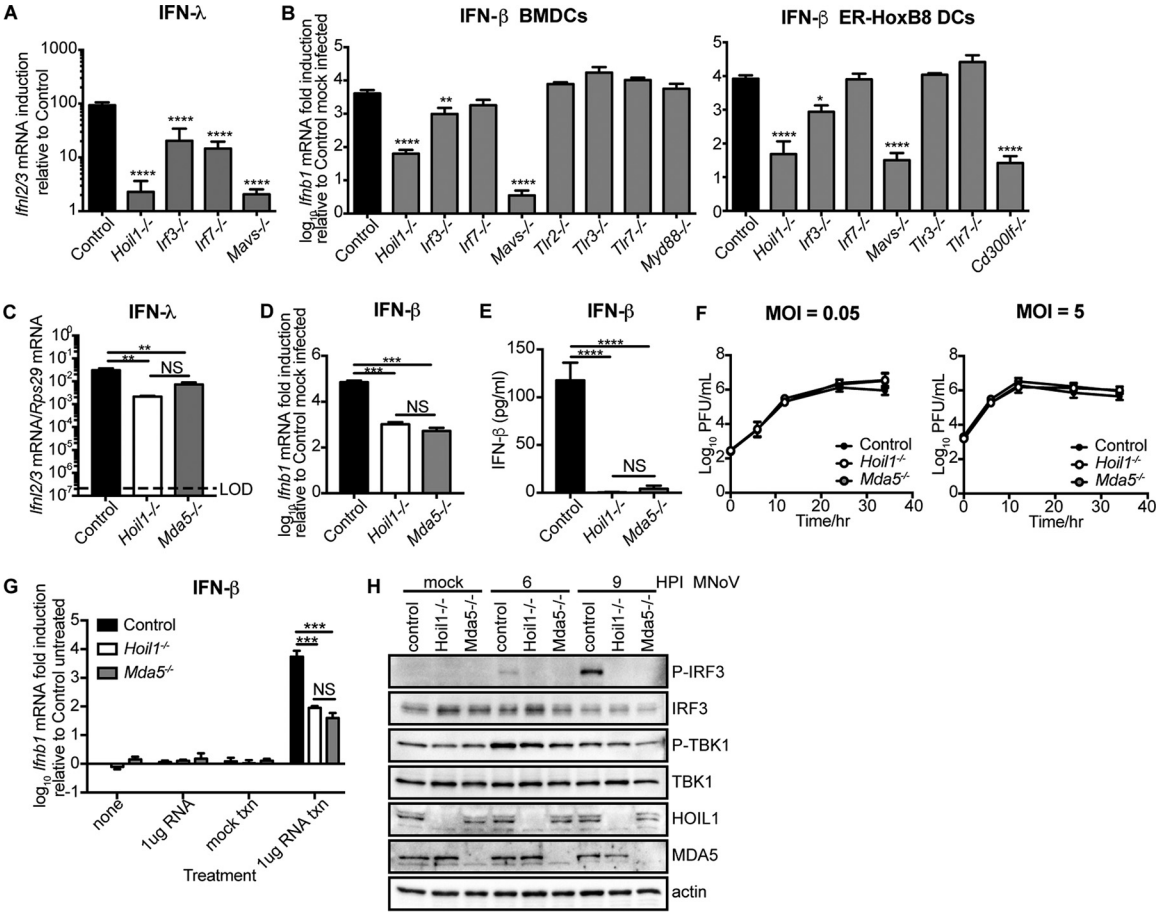

FIG 5 The MDA5-MAVS-IRF3 pathway is required for IFN-λ and IFN-β induction after MNoV infection in BMDCs. (A to D) *Ifnl2/3* (A and C) and *Ifnb1* (B and D) mRNA transcript induction in BMDCs or ER-HoxB8 DCs (B) from mice deficient in the indicated genes 10 h after infection with MNoV CR6 (MOI of 5). Data are from three to nine independent experiments. In panel A, *Ifnl2/3* expression is presented relative to induction in the WT control cells for each individual experiment. In panels A and B, results were analyzed by one-way ANOVA, with Dunnett's multiple-comparison test. Experimental groups were compared to the control group. In panel C, the dashed line shows the limit of detection (LOD). (E) IFN-β protein in control, *Hoil1*$^{-/-}$, and *Mda5*$^{-/-}$ BMDC culture supernatants 24 hpi with MNoV CR6 (MOI of 3) as measured by ELISA. Data are from three independent experiments. For panels C, D, and E, data were analyzed by one-way ANOVA with Tukey's multiple-comparison test. All groups were compared to all other groups. (F) Growth of MNoV CR6 virus in control, *Hoil1*$^{-/-}$, and *Mda5*$^{-/-}$ BMDCs infected at a low or high MOI. Values are not significantly different as determined by paired *t* test. (G) *Ifnb1* mRNA transcript induction in BMDCs from mice deficient in the indicated genes 10 h after treatment or transfection (txn) with purified MNoV virion-associated RNA. (H) Protein expression and phosphorylation in control, *Hoil1*$^{-/-}$, and *Mda5*$^{-/-}$ BMDCs at 6 and 9 hpi with MNoV CR6 and in mock-infected cells, analyzed by immunoblotting. Images are representative of three independent experiments. Values are means plus SEM. Statistical significance is indicated by asterisks as follows: *, $P < 0.05$; **, $P < 0.01$; ***, $P < 0.001$; ****, $P < 0.0001$. Values that are not significantly different are indicated (NS).

tion factors in IFN induction in response to this virus. TLR2, TLR3, TLR7, and MyD88 were dispensable for IFN-β induction after MNoV infection (Fig. 5B), supporting a primary role for the cytosolic sensors in the induction of IFNs by MNoV. ER-HoxB8 DCs generated from these knockout mice recapitulated these findings, further validating the ER-HoxB8 cell system for this study (Fig. 5B, right panel). Additionally, the defect in IFN-β induction in *Mavs*$^{-/-}$ ER-HoxB8 DCs was comparable to that observed in *Cd300lf*$^{-/-}$ cells (Fig. 5B), which lack the proteinaceous receptor essential for MNoV cell entry (63).

Next, we asked whether the RNA sensor MDA5 also plays a major role in sensing of MNoV strain CR6 and whether HOIL1 might function in this pathway. The defect in IFN-λ and IFN-β mRNA induction, as well as IFN-β protein secretion, in MDA5-deficient BMDCs after MNoV CR6 infection was not significantly different from that observed in HOIL1-deficient cells (Fig. 5C, D, and E). MNoV CR6 replicated similarly in MDA5- and HOIL1-deficient cells (Fig. 5F). To determine whether the response of these cells was due to cytoplasmic expression of viral RNA, we bypassed the entry process by trans-

fection of purified viral RNA into BMDCs followed by assessment of IFN mRNA induction. MNoV RNA induced IFN-β mRNA expression robustly in control BMDCs, and this was approximately 100-fold lower in MDA5- or HOIL1-deficient cells (Fig. 5G), indicating that intracellular sensing of viral RNA was critical for MDA5- and HOIL1-dependent IFN induction. Similar to HOIL1 deficiency, MDA5 deficiency completely abrogated the phosphorylation of IRF3 but only partially abrogated the phosphorylation of TBK1 at 6 and 9 hpi with MNoV (Fig. 5H). The absence of detected phospho-IRF3 in *Hoil1*$^{-/-}$ and *Mda5*$^{-/-}$ cells, despite a significant induction of IFN-β transcripts, implies either that IRF3 is being phosphorylated at levels below the limit of detection by immunoblotting or that the combinatorial action of several transcription factors, such as IRF1, IRF5, IRF7, and NF-κB, modulates IFN mRNA levels. Taken together, these data indicate that HOIL1 plays an essential role in the MDA5-dependent activation of IRF3 and induction of IFNs upon sensing of MNoV RNA in dendritic cells.

Virus-specific roles for HOIL1 in IFN induction in dendritic cells and fibroblasts. We considered that the discrepancy between our findings and published studies, which demonstrate that HOIL1 and LUBAC inhibit RIG-I-dependent induction of IFN during RNA virus infection, could be due to cell type-specific (i.e., dendritic cells versus fibroblasts) or virus-specific roles (i.e., MNoV versus SeV or VSV) for these proteins. To address the possibility of virus-specific roles for HOIL1 in IFN induction, we measured IFN induction in BMDCs infected with SeV or VSV, viruses with (−)ssRNA genomes known to be sensed primarily by RIG-I (17). In sharp contrast to MNoV infection, IFN-β and IFN-λ mRNA induction was almost identical in *Hoil1*$^{+/+}$ and *Hoil1*$^{-/-}$ BMDCs infected at two different multiplicities of infection (MOIs) with SeV or infected with VSV (Fig. 6A and B). These data suggest that HOIL1 is not required for IFN induction after stimulation of RIG-I. To determine whether HOIL1 is critical for IFN induction specifically after stimulation of MDA5, we infected cells with Theiler's murine encephalomyelitis virus [TMEV, which has a (+)ssRNA genome] or transfected or treated BMDCs with poly(I·C) RNA, which are sensed primarily by MDA5 (17, 54, 64). IFN mRNA induction was significantly impaired in both *Hoil1*$^{-/-}$ and *Mda5*$^{-/-}$ BMDCs after TMEV infection or poly(I·C) transfection (Fig. 6C and D). Interestingly, IFN-β induction after the addition of poly(I·C) to the cell culture medium required MDA5 and HOIL1, but IFN-λ induction did not (Fig. 6C and D). This suggests that extracellular poly(I·C) treatment activates another sensor, in addition to MDA5, that leads to preferential activation of *Ifnl2/3* promoters in a HOIL1-independent manner.

We also considered the possibility that HOIL1 may play cell type-specific roles in signaling pathways and cytokine induction, and several of the other studies of HOIL1 function have utilized fibroblasts. Therefore, we repeated the virus infections in adult skin fibroblasts isolated from the ear pinnae of control, *Hoil1*$^{-/-}$, and *Mda5*$^{-/-}$ mice. In accordance with the data obtained from BMDCs, IFN-β induction during SeV and VSV did not require HOIL1 or MDA5 (Fig. 6E). In contrast, TMEV infection, poly(I·C) RNA transfection, and MNoV RNA transfection all required both HOIL1 and MDA5 (Fig. 6E). Although fibroblasts do not express the receptor for MNoV, mCD300LF, exogenous expression of the receptor or transfection of viral cDNA permits viral replication in cell types that are not normally permissive (63, 65, 66). Addition of poly(I·C) to the fibroblast culture medium induced minimal IFN, indicating that cytosolic dsRNA is required for MDA5-dependent IFN induction in these cells. Taken together, these data strongly implicate HOIL1 as an essential component of the MDA5 signaling pathway, but not the RIG-I signaling pathway, required for the induction of type I and type III IFN after (+)ssRNA virus infection of multiple cell types.

DISCUSSION

In this study, we found that HOIL1, a component of LUBAC, is critical for the induction of type I and III IFN during infection with MNoV, a (+)ssRNA virus that induces IFNs primarily through the MDA5 signaling pathway (18). The defect in IFN transcript induction was comparable in HOIL1- and MDA5-deficient cells. Consistently, HOIL1 was required to control MNoV viral load in gastrointestinal tissues and shedding in the

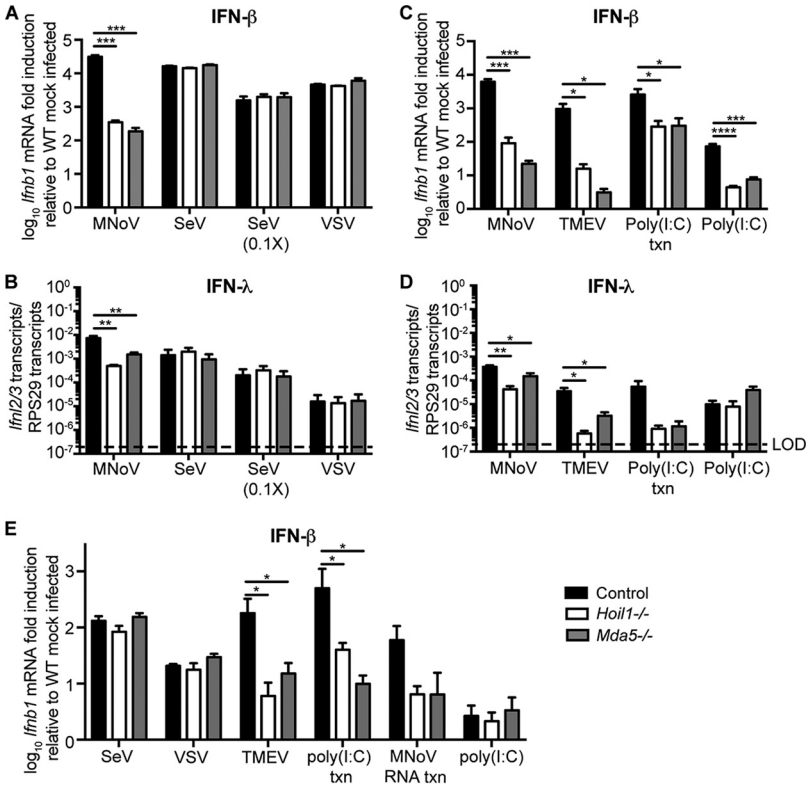

FIG 6 Virus-specific roles for HOIL1 in IFN induction in BMDCs and fibroblasts. (A to D) *Ifnb1* (A and C) and *Ifnl2/3* (B and D) mRNA transcript induction in control (black bars), *Hoil1*$^{-/-}$ (white bars), and *Mda5*$^{-/-}$ (gray bars) BMDCs after infection with MNoV CR6 (MOI of 3; 9 hpi), SeV [MOI of 3 or 0.3 (0.1×); 9 hpi], VSV (MOI of 3; 8 hpi), TMEV GDVII (MOI of 3; 8 hpi), after transfection with poly(I·C) RNA (0.1 μg/ml; 6 h) or treatment with poly(I·C) RNA (2 μg/ml; 6 h). Data are from three or four independent experiments. The dashed lines in panels B and D show the limit of detection (LOD). (E) *Ifnb1* mRNA transcript induction in control, *Hoil1*$^{-/-}$, and *Mda5*$^{-/-}$ adult ear fibroblasts after infection with SeV (MOI of 0.3; 9 hpi), VSV (MOI of 3; 9 hpi), or TMEV GDVII (MOI of 3; 8 hpi), after transfection with MNoV RNA (1 μg/ml; 10 h) or with poly(I·C) RNA (0.1 μg/ml; 6 h), or treatment with poly(I·C) RNA (2 μg/ml; 8 h). Data are from five or six independent experiments. Values are means plus SEM. All data were analyzed by one-way ANOVA, with Dunnett's multiple-comparison test. Experimental groups were compared to the control group. Statistical significance is indicated by bars and asterisks as follows: *, $P < 0.05$; **, $P < 0.01$; ***, $P < 0.001$; ****, $P < 0.0001$. txn, transfection.

stools of persistently infected mice, for the IFNLR-dependent suppression of the establishment of persistent MNoV infection by oral antibiotics (5). Furthermore, HOIL1 was required to limit acute MNoV replication and systemic infection, as well as to modulate IFN induction *in vivo*. HOIL1 was required for IFN induction in response to additional MDA5 stimuli, TMEV infection, and poly(I·C) RNA transfection (54, 64). However, we observed that HOIL1 was not required for IFN induction after RIG-I stimulation by SeV and VSV, indicating that HOIL1 plays an essential role selectively in the MDA5-dependent pathway of IFN induction. These findings identify a novel role for HOIL1 in the immune response to an RNA virus and represent the first report of a LUBAC molecule acting to stimulate a classic RNA virus-sensing pathway.

Our finding that the cytosolic RNA sensor MDA5 is critical for the recognition of MNoV strain CR6 is consistent with a prior report that MDA5 plays a major role in the induction of type I IFNs by BMDCs and in controlling viral load *in vivo* during infection with MNoV strain CW3 (18). MDA5 deficiency severely impaired induction of type I and III IFNs during infection of BMDCs with MNoV strain CR6 to an extent similar to that caused by HOIL1 deficiency. The apparent absence of a role for TLR3 *in vitro* is also consistent with this earlier study, and indeed, several other studies have also found little role for TLR3 in autonomous sensing of cells to viral infection (67, 68). Furthermore, IFN-β mRNA induction was almost completely abolished in MAVS-deficient cells,

indicating that MAVS, rather than TRIF or MyD88, is the key adaptor protein during MNoV infection of BMDCs.

While MDA5-dependent induction of IFN restricts replication of MNoV CW3 in BMDCs (18), replication of CR6 was only minimally impacted at the later stages of infection. These data may reflect differences in the sensitivity of the two viruses to type I IFN and ISGs. It is important to note that BMDCs do not express IFNLR and therefore cannot respond to IFN-λ to induce an antiviral state. Expression of IFNLR on intestinal epithelial cells (IECs) is required to restrict CR6 enteric infection, and CR6 infects tuft cells, a specialized type of IECs, *in vivo* (15, 65), as well as dendritic cells and macrophages *in vitro* (56). Additional studies will therefore be required to determine whether MDA5 and HOIL1 function to restrict MNoV CR6 replication in intestinal tuft cells.

Our initial discovery that HOIL1 is required for IFN induction via MAVS after MNoV infection contrasted with several independent studies, which found that HOIL1 and LUBAC inhibit virus-induced RIG-I signaling. One report identified both RIG-I and TRIM25 as targets for linear ubiquitination, blocking the interaction between the two proteins and marking TRIM25 for degradation during SeV infection (51). The authors utilized mouse embryonic fibroblasts (MEFs) derived from the same *Hoil1*$^{-/-}$ mouse line used in the studies presented here, eliminating the *Hoil1* targeting strategy and genetic background as potential explanations (34, 51). They reported a twofold increase in IFN-β secretion by HOIL1-deficient MEFs after SeV infection, whereas we found a 100-fold decrease in IFN-β mRNA induction during MNoV infection of BMDCs. Other studies have also reported inhibitory roles for LUBAC during SeV, VSV, or hepatitis B virus infection of fibroblasts and have identified additional proteins in the RIG-I signaling pathway as targets for linear ubiquitination, including NF-κB essential modulator (NEMO), MAVS, and IRF3 (49, 52, 53). Additionally, linear ubiquitination of IRF3 has been shown to activate the RIG-like receptor (RLR)-induced IRF3-mediated pathway of apoptosis (RIPA) as a mechanism to limit viral replication (50). In contrast to these reports, Liu et al. (69) identified only a minor role for LUBAC downstream of MAVS during VSV or SeV infection, which appeared to be redundant with another E3 ubiquitin ligase, TRAF2.

While initially perplexed by the disparity between our own data and these published reports, we subsequently observed no role for HOIL1 in IFN-β induction during SeV or VSV infection of BMDCs or adult skin fibroblasts. Therefore, we considered the possibility that differences in cytosolic receptor utilization (i.e., RIG-I versus MDA5) for sensing of RNAs from different virus types may explain the contrasting results between the various viral infection systems (70). RIG-I can bind to and aggregate around 5′-triphosphorylated RNA and the blunt end of short double-stranded RNA. In contrast, MDA5 forms filament-like structures along long double-stranded RNA and uncapped RNA in the cytosol, allowing for the recognition of different viral infections (71–73). Norovirus and picornavirus genomic RNA is uncapped and bound covalently to the viral protein VPg (74), and dsRNA replication intermediates or products are therefore likely to be a ligand for MDA5. Consistent with this model, we found that IFN induction by infection with a picornavirus, such as TMEV, or transfection with poly(I·C) RNA, required both HOIL1 and MDA5 in BMDCs and fibroblasts. Additional studies will be required to identify the specific RNA sequences and structures recognized by MDA5 during MNoV and TMEV infection. Our findings demonstrate that HOIL1 is a critical regulator of the MDA5-dependent pathway but plays a little role in the RIG-I-dependent pathway of IFN induction.

Since RIG-I and MDA5 utilize a common downstream signaling cascade, we speculate that HOIL1 functions to regulate MDA5 activation upstream of MDA5 binding to MAVS. RIG-I and MDA5 utilize several unique regulatory factors. For example, RIG-I is regulated by TRIM25, whereas MDA5 appears to be regulated by LGP2 (75, 76). However, the previously identified targets for linear ubiquitination, MAVS, NEMO, and IRF3, are common to both RLR pathways, and a report indicating a redundant function with TRAF2 also places LUBAC downstream of MAVS (69). LUBAC may therefore be required for the MDA5-dependent activation of MAVS, as well as to modulate signaling

events at downstream steps to ensure tight regulation of the RLR pathways and IFN production.

One potential caveat to our findings is that the cell types used in this study express truncated forms of HOIL1, albeit at levels lower than that of the full-length protein in wild-type cells. Even though the cells derived from the mouse and by CRISPR/Cas9 mutagenesis express different protein products and are associated with partial destabilization of LUBAC, we cannot completely rule out the possibility that the truncated forms of HOIL1 that lack the RING domains possess an aberrant function. Since complete HOIL1 deficiency is embryonic lethal in mice, future studies with cell type-specific deletion of *Hoil1* will be critical to fully elucidate the roles of HOIL1 *in vivo* and *in vitro*.

Together, our findings demonstrate a novel role for HOIL1 in the sensing of viral infection and induction of IFNs and suggest that HOIL1 may be important for IFN induction to limit replication of a broad array of (+)ssRNA viruses sensed by MDA5. Further studies will be required to identify the relevant targets of HOIL1 and LUBAC in the MDA5 signaling pathway and to dissect the apparently divergent roles of the LUBAC during diverse viral infections.

MATERIALS AND METHODS

Generation of viral stocks and titers. Stocks of MNoV strains CR6 and CW3 were generated from molecular clones as previously described (63, 77). Briefly, a plasmid carrying the MNoV CR6 or CW3 genome was transfected into 293T cells to generate infectious virus, which was subsequently passaged on BV2 cells. After two passages, BV2 cultures were frozen and thawed to liberate virions. Then, cultures were cleared of cellular debris and concentrated by ultracentrifugation, pelleted through a 30% sucrose cushion. The titers of MNoV stocks were determined by plaque assay on BV2 cells (63, 77). Sendai virus Cantell strain was obtained from ATCC (VR-907) and used to infect BMDCs directly. VSV labeled with green fluorescent protein (VSV-GFP) (78) and TMEV strain GDVII were propagated in Vero cells and BHK cells, respectively, and purified by filtration of cell culture supernatant through a 0.22-μm filter. The titers of VSV-GFP and TMEV stocks were determined by plaque assay on Vero cells and BHK cells, respectively.

Mice, infections, and treatments. C57BL/6J mice (catalog no. 000664) were purchased from Jackson Laboratories (Bar Harbor, ME) and housed at Washington University School of Medicine and the University of Illinois at Chicago College of Medicine under specific-pathogen-free conditions according to university guidelines. Knockout mice on the C57BL/6J background were maintained under the same conditions. *Hoil1*$^{-/-}$ mice, with null mutations in the *Rbck1* gene that encodes HOIL1, have been described previously (34). Age- and sex-matched C57BL/6J mice or *Hoil1*$^{+/+}$ littermates were used as wild-type controls for *in vivo* experiments. Additional mouse strains included the following: *Stat1*$^{-/-}$ (B6.129-Stat1tm1Dlv) (79), *Tlr2*$^{-/-}$ (JAX B6.129-Tlr2tm1Kir/J; catalog no. 004650) (80), *Tlr3*$^{-/-}$ (B6;129S1-Tlr3tm1Flv/J; catalog no. 005217) (81), *Tlr7*$^{-/-}$ (B6.129S1-Tlr7tm1Flv/J; catalog no. 008380) (82), *Myd88*$^{-/-}$ [JAX B6.129P2(SJL)-Myd88tm1.1Defr/J; catalog no. 009088] (83), *Mavs*$^{-/-}$ (B6;129-Mavstm1Zjc/Jlrf3$^{-/-}$; catalog no. 008634) (84), *Irf3*$^{-/-}$ (B6.129S/SvEv-Bcl2l12/Irf3tm1Ttg) (85), *Irf7*$^{-/-}$ (B6.129P2-Irf7tm1Ttg/TtgRbrc) (86), and *Mda5*$^{-/-}$ (B6.Cg-Ifih1tm1.1Cln/J; catalog no. 015812) (64) mice. Cas9 knock-in mice [B6;129-Gt(ROSA)26Sortm1(CAG-cas9*,-EGFP)Fezh/J; catalog no. 024857] (87) were bred to Deleter-cre mice to enable constitutive expression of Cas9. *Cd300lf*$^{-/-}$ mice have been described previously (63). Both males and females were used.

Six-week-old mice were treated with an antibiotic cocktail (1 g/liter ampicillin, 1 g/liter metronidazole, 1 g/liter neomycin, 0.5 g/liter vancomycin [Sigma, St. Louis, MO]) in 20 g/liter grape Kool-Aid (Kraft Foods, Northfield, IL) or with Kool-Aid alone for 2 weeks prior to inoculation with virus as described previously (5). The mice were inoculated orally with 10^6 PFU of MNoV strain CR6 or strain CW3 in 25 μl of Dulbecco modified Eagle medium (DMEM). Recombinant IFN-λ was provided by Bristol-Myers Squibb (Seattle, WA) as a monomeric conjugate comprised of 20-kDa linear polyethylene glycol (PEG) attached to the amino terminus of murine IFN-λ, as previously reported (7). Mice were treated by intraperitoneal injection of 25 μg IFN-λ diluted in phosphate-buffered saline (PBS) or PBS alone. Stool samples and tissues from euthanized mice were harvested into sterile 2-ml O-ring tubes containing 1-mm-diameter zirconia/silica beads (Biospec, Bartlesville, OK). Tissues were flash frozen in a bath of ethanol and dry ice and either processed on the same day or stored at −80°C.

Cell culture and infections. Bone marrow-derived dendritic cells (BMDCs) were differentiated in RPMI 1640 (Corning) supplemented with 10% fetal bovine serum (FBS), 1% L-glutamine, 1% HEPES, and 2% conditioned medium containing GM-CSF at 37°C with 5% CO_2 in a humidified incubator for 7 days. For RNA and protein analyses, nonadherent cells were harvested and infected with MNoV strain CR6 at a multiplicity of infection (MOI) of 3 to 5 (as indicated), with SeV at an MOI of 3 or 0.3 (3 or 0.3 50% egg (or egg embryo) infectious dose [EID_{50}]/cell), with VSV-GFP or TMEV at an MOI of 3 or mock infected and replated in tissue culture-treated dishes in medium without GM-CSF. To determine IFN protein levels in the cell supernatant, cells were infected with MNoV or mock infected as described above and plated at the same density in 96-well plates. Cell supernatants were harvested at 12 and 24 hpi and stored at −80°C. For treatment or transfection with purified MNoV RNA or poly(I·C), day 7 BMDCs were harvested and replated in medium containing GM-CSF in tissue culture dishes at 2.5×10^5 cells per well. Twenty

hours later, cells were mock treated or treated with 1 μg MNoV RNA or 2 μg poly(I·C) (Invivogen). The cells were mock transfected or transfected with 1 μg MNoV RNA or 0.1 μg poly(I·C) using TransIT mRNA transfection kit (Mirus). MNoV RNA for transfection was isolated from purified MNoV stocks using TRIzol-LS (Invitrogen) and treated with DNase (Ambion DNA-free kit).

Murine adult skin fibroblasts were isolated from the ear pinnae of 8- to 12-week-old mice. Ear pinnae were cut into small pieces in Hanks' buffered salt solution, digested sequentially with collagenase (type XI-S; Sigma-Aldrich) and trypsin, and passed through a 100-μm cell strainer. Isolated cells were cultured in DMEM supplemented with 10% FBS, 1% L-glutamine, 0.5% penicillin-streptomycin. Fibroblasts were plated in 12-well plates at 10^5 cells/well, and 20 h later, the fibroblasts were infected with SeV (MOI of 0.3), VSV-GFP (MOI of 3), or TMEV GDVII (MOI of 3) or treated or transfected with MNoV RNA or poly(I·C) as described above for BMDCs.

At the indicated time points, the media were removed, and the cells were lysed in Tri Reagent (Sigma-Aldrich) for RNA isolation and stored at −80°C or lysed in 2× Laemmli buffer for Western blot analysis, boiled for 10 min, and stored at −20°C.

For single and multistep viral growth curves, day 7 BMDCs were infected with MNoV at an MOI of 5 or 0.05, incubated on ice for 30 min, washed three times with fresh media, and replated in 24-well tissue culture-treated dishes. Dishes were transferred to −80°C at the indicated time points. Viral titers were determined by plaque assay on BV2 cell monolayers (63).

ER-HoxB8 cell generation, CRISPR/Cas9 KO, and cell differentiation. ER-HoxB8 precursor cells were generated as described in the original methods paper (60). Briefly, bone marrow cells were isolated over a Ficoll-plaque gradient, and transduced with a murine stem cell virus (MSCV)-based retrovirus expressing a mouse Hoxb8-estrogen receptor (ER) fusion protein (produced in PLAT-E producer cells). Transduced cells were grown in RPMI 1640 supplemented with 10% FBS, 1% L-glutamine, 1% HEPES, 1% penicillin-streptomycin, 20 ng/ml GM-CSF (Peprotech) and 1 μm β-estradiol (Sigma-Aldrich) for at least 4 weeks.

To generate a HOIL1 knockout (KO) cell line using CRISPR/Cas9-based methods, guide RNAs were designed using the sgRNA designer tool from the Genetic Perturbation Platform at the Broad Institute. Oligonucleotides encoding an sgRNA predicted to target HOIL1 exon 6 (TGC TTC ATA CCA GCC TGA CG) were cloned into pLentiGuide-Puro (Addgene) (88, 89). Lentiviral particles were produced in 293T cells by cotransfection of this plasmid with pMD2-G and psPAX2 and used to transduce ER-HoxB8 precursor cells generated from a Cas9-expressing mouse (87). Transduced cells were selected with 6 μg/ml puromycin. Individual puromycin-resistant cells were subcloned by limiting dilutions and screened for loss of HOIL1 expression by Western blotting.

To differentiate ER-HoxB8 precursor cells into DCs, cells were washed twice with RPMI 1640 complete medium (without GM-CSF or β-estradiol) to remove the β-estradiol, then plated, and grown in RPMI 1640 complete medium with 2% conditioned media containing GM-CSF for 7 days as described above for primary BMDCs.

Quantitation of viral genome copies and cellular gene expression by quantitative reverse transcription-PCR. RNA from stool samples was isolated using a ZR-96 viral RNA kit (Zymo Research, Irvine, CA). RNA from tissues was isolated using Tri Reagent (Sigma-Aldrich) and a Direct-zol-96 RNA kit (Zymo Research, Irvine, CA) according to the manufacturer's protocol. RNA from cultured cells was isolated using Tri Reagent according to the manufacturer's protocol. RNA isolated from cells was treated with DNase (Ambion DNA-free kit) prior to cDNA synthesis. Five microliters of RNA from stool or 1 μg of RNA from tissue or cells was used as a template for cDNA synthesis with ImProm-II reverse transcriptase (Promega, Madison, WI). MNoV TaqMan qPCR assays were performed as described previously (90). Quantitative PCR (qPCR) for *Ifnb1* and *Hoil1/Rbck1* was performed using predesigned 5′ nuclease probe-based assays Mm.PT.58.30132453.g and Mm.PT.58.30767649, respectively (Integrated DNA Technologies). *Ifnl2/3* transcripts were detected using predesigned probe-based assay Mm04204156_gH (Applied Biosystems). MNoV genome quantities from tissue samples and IFN transcripts were normalized to housekeeping gene ribosomal protein S29 (*Rps29*). When possible, a $\Delta\Delta C_T$ analysis was performed and presented as fold change relative to the values for mock-infected cells. *Ifnl2/3* transcripts were not detected in untreated cells and therefore presented as *Ifnl2/3* transcripts/*Rps29* transcripts. qPCR for *Rps29* was performed with forward primer 5′-GCA AAT ACG GGC TGA ACA TG-3′, reverse primer 5′-GTC CAA CTT AAT GAA GCC TAT GTC-3′, and probe 5′-/5HEX/CCT TCG CGT/ZEN/ACT GCC GGA AGC/3IABkFQ/-3′ (Integrated DNA Technologies), using AmpliTaq Gold DNA polymerase (Applied Biosystems). qPCR standards were generated using ORFeome Collaboration *Mus musculus Ifnl3* open reading frame (ORF) clone identifier (ID) 100014638 (Dharmacon) for *Ifnl2/3*, and a gene block containing the sequence TTTTTCACGCCACCGATCTGTTCTGCGCTGGGTGCGCTTTGGAACAATGGATGCTGAGAC CCCGCAGGAACGCTCAGCAGTCTTTGTGAATGAGGATGAGTGATGGCGCAGCGCTTTTTGCAAATACGGGCTGAAC ATGTGCCGCCAGTGCTTCCGGCAGTACGCGAAGGACATAGGCTTCATTAAGTTGGACTTTTT for *Rps29* and MNoV (Integrated DNA Technologies).

Immunoblot analyses. Cells were lysed in 2× Laemmli buffer (4% SDS, 10% β-mercaptoethanol, 20% glycerol, 0.004% bromophenol blue, and 0.125 M Tris-HCl [pH 6.8], 2× Halt protease, and phosphate inhibitor [Thermo Fisher Scientific] was added immediately before use), boiled for 10 min, and stored at −20°C. Proteins were separated by SDS-PAGE, transferred to a polyvinylidene difluoride (PVDF) membrane, blocked with either 5% bovine serum albumin (BSA), or 1% or 5% nonfat dried milk in Tris-buffered saline (TBS) containing 0.1% Tween 20. The membranes were incubated with the following primary antibodies: anti-HOIL1 (NBP1-883001; Novus Bio), anti-phospho-IRF3 (29047S; Cell Signaling Technology), anti-IRF3 (ab68481;Abcam), anti-phospho-TBK1 (5483S; Cell Signaling Technology), anti-TBK1 (3504S; Cell Signaling Technology), anti-MDA5 (AL180; AdipoGen), anti-beta-actin (A5316; Sigma-Aldrich), anti-SHARPIN (14626-1-AP; Proteintech), and anti-MAVS (ab31334; Abcam). This was followed by incubation with the appropriate secondary antibody: goat anti-rabbit IgG conjugated to horseradish

peroxidase (HRP) (goat anti-rabbit IgG-HRP) and goat anti-mouse IgG-HRP (Jackson Immunoresearch). Blots were incubated with Immobilon Western chemiluminescent HRP substrate (Millipore) and imaged on a ChemiDoc Imaging System (Bio-Rad).

Flow cytometry. BMDC and ER-HoxB8-DC differentiation was confirmed by staining for cell surface markers CD11b (M1/70; eBioscience) and CD11c (N418; eBioscience) and analysis on an LSR-Fortessa flow cytometer (BD Biosciences).

Quantification of IFN protein in cell supernatants. Mouse IFN (mIFN-β) and mIFN-λ protein levels in cell supernatants were quantified by ELISA (R&D Systems) according to the manufacturer's instructions.

Statistical analyses. Data were analyzed with Prism 6 software (GraphPad Software, San Diego, CA). Statistical significance was determined by unpaired *t* test, Mann-Whitney test, one-way analysis of variance (ANOVA) with Tukey's multiple-comparison test, or two-way ANOVA with Sidak's multiple-comparison test as indicated in the figure legends.

ACKNOWLEDGMENTS

We thank D. Kreamalmeyer for animal care and breeding, M. Wood and members of the Virgin laboratory for manuscript reviews and discussions, C. S. Hsieh (Washington University) for providing the Cas9 knock-in mice crossed with Deleter-cre mice, M. P. Kamps (University of California, San Diego [UCSD)] for providing the HoxB8 expression system, R. Orchard for the *Cd300lf*$^{-/-}$ ER-HoxB8 cells, H. Lipton for TMEV strain GDVII, S. Whelan and N. Sarute for VSV-GFP, and S. Garrett for initiating the SeV study.

H.W.V. was supported by National Institutes of Health (NIH) grant R01 U19AI109725, Crohn's and Colitis Foundation Genetics Initiative grant 326556. M.T.B. was supported by NIH training grant 5T32CA009547 and NIH K22AI127846. T.J.N. was supported by NIH training grant 5T32A100716334 and postdoctoral fellowships from the American Cancer Society.

The funders had no role in study design, data collection and interpretation, or the decision to submit the work for publication.

REFERENCES

1. Cardemil CV, Parashar UD, Hall AJ. 2017. Norovirus infection in older adults: epidemiology, risk factors, and opportunities for prevention and control. Infect Dis Clin North Am 31:839–870. https://doi.org/10.1016/j.idc.2017.07.012.
2. Patel MM, Widdowson MA, Glass RI, Akazawa K, Vinje J, Parashar UD. 2008. Systematic literature review of role of noroviruses in sporadic gastroenteritis. Emerg Infect Dis 14:1224–1231. https://doi.org/10.3201/eid1408.071114.
3. Baldridge MT, Turula H, Wobus CE. 2016. Norovirus regulation by host and microbe. Trends Mol Med 22:1047–1059. https://doi.org/10.1016/j.molmed.2016.10.003.
4. Karst SM, Wobus CE, Goodfellow IG, Green KY, Virgin HW. 2014. Advances in norovirus biology. Cell Host Microbe 15:668–680. https://doi.org/10.1016/j.chom.2014.05.015.
5. Baldridge MT, Nice TJ, McCune BT, Yokoyama CC, Kambal A, Wheadon M, Diamond MS, Ivanova Y, Artyomov M, Virgin HW. 2015. Commensal microbes and interferon-lambda determine persistence of enteric murine norovirus infection. Science 347:266–269. https://doi.org/10.1126/science.1258025.
6. Jones MK, Watanabe M, Zhu S, Graves CL, Keyes LR, Grau KR, Gonzalez-Hernandez MB, Iovine NM, Wobus CE, Vinje J, Tibbetts SA, Wallet SM, Karst SM. 2014. Enteric bacteria promote human and mouse norovirus infection of B cells. Science 346:755–759. https://doi.org/10.1126/science.1257147.
7. Nice TJ, Baldridge MT, McCune BT, Norman JM, Lazear HM, Artyomov M, Diamond MS, Virgin HW. 2015. Interferon-lambda cures persistent murine norovirus infection in the absence of adaptive immunity. Science 347:269–273. https://doi.org/10.1126/science.1258100.
8. Kawai T, Akira S. 2006. Innate immune recognition of viral infection. Nat Immunol 7:131–137. https://doi.org/10.1038/ni1303.
9. Schindler C, Plumlee C. 2008. Inteferons pen the JAK-STAT pathway. Semin Cell Dev Biol 19:311–318. https://doi.org/10.1016/j.semcdb.2008.08.010.
10. Andreakos E, Salagianni M, Galani IE, Koltsida O. 2017. Interferon-lambdas: front-line guardians of immunity and homeostasis in the respiratory tract. Front Immunol 8:1232. https://doi.org/10.3389/fimmu.2017.01232.
11. Lee S, Baldridge MT. 2017. Interferon-lambda: a potent regulator of intestinal viral infections. Front Immunol 8:749. https://doi.org/10.3389/fimmu.2017.00749.
12. Pott J, Stockinger S. 2017. Type I and III interferon in the gut: tight balance between host protection and immunopathology. Front Immunol 8:258. https://doi.org/10.3389/fimmu.2017.00258.
13. Karst SM, Wobus CE, Lay M, Davidson J, Virgin HW. 2003. STAT1-dependent innate immunity to a Norwalk-like virus. Science 299:1575–1578. https://doi.org/10.1126/science.1077905.
14. Nice TJ, Osborne LC, Tomov VT, Artis D, Wherry EJ, Virgin HW. 2016. Type I interferon receptor deficiency in dendritic cells facilitates systemic murine norovirus persistence despite enhanced adaptive immunity. PLoS Pathog 12:e1005684. https://doi.org/10.1371/journal.ppat.1005684.
15. Baldridge MT, Lee S, Brown JJ, McAllister N, Urbanek K, Dermody TS, Nice TJ, Virgin HW. 2017. Expression of Ifnlr1 on intestinal epithelial cells is critical to the antiviral effects of interferon lambda against norovirus and reovirus. J Virol 91:e02079-16. https://doi.org/10.1128/JVI.02079-16.
16. Loo YM, Gale M, Jr. 2011. Immune signaling by RIG-I-like receptors. Immunity 34:680–692. https://doi.org/10.1016/j.immuni.2011.05.003.
17. Jensen S, Thomsen AR. 2012. Sensing of RNA viruses: a review of innate immune receptors involved in recognizing RNA virus invasion. J Virol 86:2900–2910. https://doi.org/10.1128/JVI.05738-11.
18. McCartney SA, Thackray LB, Gitlin L, Gilfillan S, Virgin HW, IV, Colonna M. 2008. MDA-5 recognition of a murine norovirus. PLoS Pathog 4:e1000108. https://doi.org/10.1371/journal.ppat.1000108.
19. Thackray LB, Duan E, Lazear HM, Kambal A, Schreiber RD, Diamond MS, Virgin HW. 2012. Critical role for interferon regulatory factor 3 (IRF-3) and IRF-7 in type I interferon-mediated control of murine norovirus replication. J Virol 86:13515–13523. https://doi.org/10.1128/JVI.01824-12.
20. Heaton SM, Borg NA, Dixit VM. 2016. Ubiquitin in the activation and attenuation of innate antiviral immunity. J Exp Med 213:1–13. https://doi.org/10.1084/jem.20151531.
21. Zinngrebe J, Montinaro A, Peltzer N, Walczak H. 2014. Ubiquitin in the immune system. EMBO Rep 15:28–45. https://doi.org/10.1002/embr.201338025.
22. Shimizu Y, Taraborrelli L, Walczak H. 2015. Linear ubiquitination in immunity. Immunol Rev 266:190–207. https://doi.org/10.1111/imr.12309.
23. MacDuff DA, Reese TA, Kimmey JM, Weiss LA, Song C, Zhang X, Kambal A, Duan E, Carrero JA, Boisson B, Laplantine E, Israel A, Picard C, Colonna

M, Edelson BT, Sibley LD, Stallings CL, Casanova JL, Iwai K, Virgin HW. 2015. Phenotypic complementation of genetic immunodeficiency by chronic herpesvirus infection. Elife 4:e04494. https://doi.org/10.7554/eLife.04494.
24. Boisson B, Laplantine E, Dobbs K, Cobat A, Tarantino N, Hazen M, Lidov HG, Hopkins G, Du L, Belkadi A, Chrabieh M, Itan Y, Picard C, Fournet JC, Eibel H, Tsitsikov E, Pai SY, Abel L, Al-Herz W, Casanova JL, Israel A, Notarangelo LD. 2015. Human HOIP and LUBAC deficiency underlies autoinflammation, immunodeficiency, amylopectinosis, and lymphangiectasia. J Exp Med 212:939–951. https://doi.org/10.1084/jem.20141130.
25. Walczak H, Iwai K, Dikic I. 2012. Generation and physiological roles of linear ubiquitin chains. BMC Biol 10:23. https://doi.org/10.1186/1741-7007-10-23.
26. Boisson B, Laplantine E, Prando C, Giliani S, Israelsson E, Xu Z, Abhyankar A, Israel L, Trevejo-Nunez G, Bogunovic D, Cepika AM, MacDuff D, Chrabieh M, Hubeau M, Bajolle F, Debre M, Mazzolari E, Vairo D, Agou F, Virgin HW, Bossuyt X, Rambaud C, Facchetti F, Bonnet D, Quartier P, Fournet JC, Pascual V, Chaussabel D, Notarangelo LD, Puel A, Israel A, Casanova JL, Picard C. 2012. Immunodeficiency, autoinflammation and amylopectinosis in humans with inherited HOIL-1 and LUBAC deficiency. Nat Immunol 13:1178–1186. https://doi.org/10.1038/ni.2457.
27. Gerlach B, Cordier SM, Schmukle AC, Emmerich CH, Rieser E, Haas TL, Webb AI, Rickard JA, Anderton H, Wong WW, Nachbur U, Gangoda L, Warnken U, Purcell AW, Silke J, Walczak H. 2011. Linear ubiquitination prevents inflammation and regulates immune signalling. Nature 471:591–596. https://doi.org/10.1038/nature09816.
28. Wang Z, Potter CS, Sundberg JP, Hogenesch H. 2012. SHARPIN is a key regulator of immune and inflammatory responses. J Cell Mol Med 16:2271–2279. https://doi.org/10.1111/j.1582-4934.2012.01574.x.
29. Zak DE, Schmitz F, Gold ES, Diercks AH, Peschon JJ, Valvo JS, Niemisto A, Podolsky I, Fallen SG, Suen R, Stolyar T, Johnson CD, Kennedy KA, Hamilton MK, Siggs OM, Beutler B, Aderem A. 2011. Systems analysis identifies an essential role for SHANK-associated RH domain-interacting protein (SHARPIN) in macrophage Toll-like receptor 2 (TLR2) responses. Proc Natl Acad Sci U S A 108:11536–11541. https://doi.org/10.1073/pnas.1107577108.
30. Tokunaga F, Nakagawa T, Nakahara M, Saeki Y, Taniguchi M, Sakata S, Tanaka K, Nakano H, Iwai K. 2011. SHARPIN is a component of the NF-kappaB-activating linear ubiquitin chain assembly complex. Nature 471:633–636. https://doi.org/10.1038/nature09815.
31. Ikeda F, Deribe YL, Skanland SS, Stieglitz B, Grabbe C, Franz-Wachtel M, van Wijk SJ, Goswami P, Nagy V, Terzic J, Tokunaga F, Androulidaki A, Nakagawa T, Pasparakis M, Iwai K, Sundberg JP, Schaefer L, Rittinger K, Macek B, Dikic I. 2011. SHARPIN forms a linear ubiquitin ligase complex regulating NF-kappaB activity and apoptosis. Nature 471:637–641. https://doi.org/10.1038/nature09814.
32. Stieglitz B, Morris-Davies AC, Koliopoulos MG, Christodoulou E, Rittinger K. 2012. LUBAC synthesizes linear ubiquitin chains via a thioester intermediate. EMBO Rep 13:840–846. https://doi.org/10.1038/embor.2012.105.
33. Smit JJ, Monteferrario D, Noordermeer SM, van Dijk WJ, van der Reijden BA, Sixma TK. 2012. The E3 ligase HOIP specifies linear ubiquitin chain assembly through its RING-IBR-RING domain and the unique LDD extension. EMBO J 31:3833–3844. https://doi.org/10.1038/emboj.2012.217.
34. Tokunaga F, Sakata S, Saeki Y, Satomi Y, Kirisako T, Kamei K, Nakagawa T, Kato M, Murata S, Yamaoka S, Yamamoto M, Akira S, Takao T, Tanaka K, Iwai K. 2009. Involvement of linear polyubiquitylation of NEMO in NF-kappaB activation. Nat Cell Biol 11:123–132. https://doi.org/10.1038/ncb1821.
35. Kirisako T, Kamei K, Murata S, Kato M, Fukumoto H, Kanie M, Sano S, Tokunaga F, Tanaka K, Iwai K. 2006. A ubiquitin ligase complex assembles linear polyubiquitin chains. EMBO J 25:4877–4887. https://doi.org/10.1038/sj.emboj.7601360.
36. Popovic D, Vucic D, Dikic I. 2014. Ubiquitination in disease pathogenesis and treatment. Nat Med 20:1242–1253. https://doi.org/10.1038/nm.3739.
37. Elton L, Carpentier I, Verhelst K, Staal J, Beyaert R. 2015. The multifaceted role of the E3 ubiquitin ligase HOIL-1: beyond linear ubiquitination. Immunol Rev 266:208–221. https://doi.org/10.1111/imr.12307.
38. Wang K, Kim C, Bradfield J, Guo Y, Toskala E, Otieno FG, Hou C, Thomas K, Cardinale C, Lyon GJ, Golhar R, Hakonarson H. 2013. Whole-genome DNA/RNA sequencing identifies truncating mutations in RBCK1 in a novel Mendelian disease with neuromuscular and cardiac involvement. Genome Med 5:67. https://doi.org/10.1186/gm471.
39. Nilsson J, Schoser B, Laforet P, Kalev O, Lindberg C, Romero NB, Davila Lopez M, Akman HO, Wahbi K, Iglseder S, Eggers C, Engel AG, Dimauro S, Oldfors A. 2013. Polyglucosan body myopathy caused by defective ubiquitin ligase RBCK1. Ann Neurol 74:914–919. https://doi.org/10.1002/ana.23963.
40. Peltzer N, Rieser E, Taraborrelli L, Draber P, Darding M, Pernaute B, Shimizu Y, Sarr A, Draberova H, Montinaro A, Martinez-Barbera JP, Silke J, Rodriguez TA, Walczak H. 2014. HOIP deficiency causes embryonic lethality by aberrant TNFR1-mediated endothelial cell death. Cell Rep 9:153–165. https://doi.org/10.1016/j.celrep.2014.08.066.
41. Rickard JA, Anderton H, Etemadi N, Nachbur U, Darding M, Peltzer N, Lalaoui N, Lawlor KE, Vanyai H, Hall C, Bankovacki A, Gangoda L, Wong WW, Corbin J, Huang C, Mocarski ES, Murphy JM, Alexander WS, Voss AK, Vaux DL, Kaiser WJ, Walczak H, Silke J. 2014. TNFR1-dependent cell death drives inflammation in Sharpin-deficient mice. Elife 3:e03464. https://doi.org/10.7554/eLife.03464.
42. Seymour RE, Hasham MG, Cox GA, Shultz LD, Hogenesch H, Roopenian DC, Sundberg JP. 2007. Spontaneous mutations in the mouse Sharpin gene result in multiorgan inflammation, immune system dysregulation and dermatitis. Genes Immun 8:416–421. https://doi.org/10.1038/sj.gene.6364403.
43. Zinngrebe J, Rieser E, Taraborrelli L, Peltzer N, Hartwig T, Ren H, Kovacs I, Endres C, Draber P, Darding M, von Karstedt S, Lemke J, Dome B, Bergmann M, Ferguson BJ, Walczak H. 2016. LUBAC deficiency perturbs TLR3 signaling to cause immunodeficiency and autoinflammation. J Exp Med 213:2671–2689. https://doi.org/10.1084/jem.20160041.
44. Peltzer N, Darding M, Montinaro A, Draber P, Draberova H, Kupka S, Rieser E, Fisher A, Hutchinson C, Taraborrelli L, Hartwig T, Lafont E, Haas TL, Shimizu Y, Boiers C, Sarr A, Rickard J, Alvarez-Diaz S, Ashworth MT, Beal A, Enver T, Bertin J, Kaiser W, Strasser A, Silke J, Bouillet P, Walczak H. 2018. LUBAC is essential for embryogenesis by preventing cell death and enabling haematopoiesis. Nature 557:112–117. https://doi.org/10.1038/s41586-018-0064-8.
45. Fujita H, Tokunaga A, Shimizu S, Whiting AL, Aguilar-Alonso F, Takagi K, Walinda E, Sasaki Y, Shimokawa T, Mizushima T, Ohki I, Ariyoshi M, Tochio H, Bernal F, Shirakawa M, Iwai K. 2018. Cooperative domain formation by homologous motifs in HOIL-1L and SHARPIN plays a crucial role in LUBAC stabilization. Cell Rep 23:1192–1204. https://doi.org/10.1016/j.celrep.2018.03.112.
46. Fiil BK, Gyrd-Hansen M. 2014. Met1-linked ubiquitination in immune signalling. FEBS J 281:4337–4350. https://doi.org/10.1111/febs.12944.
47. Sasaki K, Iwai K. 2015. Roles of linear ubiquitinylation, a crucial regulator of NF-kappaB and cell death, in the immune system. Immunol Rev 266:175–189. https://doi.org/10.1111/imr.12308.
48. Rodgers MA, Bowman JW, Fujita H, Orazio N, Shi M, Liang Q, Amatya R, Kelly TJ, Iwai K, Ting J, Jung JU. 2014. The linear ubiquitin assembly complex (LUBAC) is essential for NLRP3 inflammasome activation. J Exp Med 211:1333–1347. https://doi.org/10.1084/jem.20132486.
49. Belgnaoui SM, Paz S, Samuel S, Goulet ML, Sun Q, Kikkert M, Iwai K, Dikic I, Hiscott J, Lin R. 2012. Linear ubiquitination of NEMO negatively regulates the interferon antiviral response through disruption of the MAVS-TRAF3 complex. Cell Host Microbe 12:211–222. https://doi.org/10.1016/j.chom.2012.06.009.
50. Chattopadhyay S, Kuzmanovic T, Zhang Y, Wetzel JL, Sen GC. 2016. Ubiquitination of the transcription factor IRF-3 activates RIPA, the apoptotic pathway that protects mice from viral pathogenesis. Immunity 44:1151–1161. https://doi.org/10.1016/j.immuni.2016.04.009.
51. Inn KS, Gack MU, Tokunaga F, Shi M, Wong LY, Iwai K, Jung JU. 2011. Linear ubiquitin assembly complex negatively regulates RIG-I- and TRIM25-mediated type I interferon induction. Mol Cell 41:354–365. https://doi.org/10.1016/j.molcel.2010.12.029.
52. Khan M, Syed GH, Kim SJ, Siddiqui A. 2016. Hepatitis B virus-induced Parkin-dependent recruitment of linear ubiquitin assembly complex (LUBAC) to mitochondria and attenuation of innate immunity. PLoS Pathog 12:e1005693. https://doi.org/10.1371/journal.ppat.1005693.
53. Zhang M, Tian Y, Wang RP, Gao D, Zhang Y, Diao FC, Chen DY, Zhai ZH, Shu HB. 2008. Negative feedback regulation of cellular antiviral signaling by RBCK1-mediated degradation of IRF3. Cell Res 18:1096–1104. https://doi.org/10.1038/cr.2008.277.
54. Jin YH, Kim SJ, So EY, Meng L, Colonna M, Kim BS. 2012. Melanoma differentiation-associated gene 5 is critical for protection against Theiler's virus-induced demyelinating disease. J Virol 86:1531–1543. https://doi.org/10.1128/JVI.06457-11.
55. Elftman MD, Gonzalez-Hernandez MB, Kamada N, Perkins C, Henderson

KS, Núñez G, Wobus CE. 2013. Multiple effects of dendritic cell depletion on murine norovirus infection. J Gen Virol 94:1761–1768. https://doi.org/10.1099/vir.0.052134-0.
56. Wobus CE, Karst SM, Thackray LB, Chang KO, Sosnovtsev SV, Belliot G, Krug A, Mackenzie JM, Green KY, Virgin HW. 2004. Replication of Norovirus in cell culture reveals a tropism for dendritic cells and macrophages. PLoS Biol 2:e432. https://doi.org/10.1371/journal.pbio.0020432.
57. Grau KR, Roth AN, Zhu S, Hernandez A, Colliou N, DiVita BB, Philip DT, Riffe C, Giasson B, Wallet SM, Mohamadzadeh M, Karst SM. 2017. The major targets of acute norovirus infection are immune cells in the gut-associated lymphoid tissue. Nat Microbiol 2:1586–1591. https://doi.org/10.1038/s41564-017-0057-7.
58. Rathinam VA, Fitzgerald KA. 2011. Cytosolic surveillance and antiviral immunity. Curr Opin Virol 1:455–462. https://doi.org/10.1016/j.coviro.2011.11.004.
59. Thackray LB, Wobus CE, Chachu KA, Liu B, Alegre ER, Henderson KS, Kelley ST, Virgin HW. 2007. Murine noroviruses comprising a single genogroup exhibit biological diversity despite limited sequence divergence. J Virol 81:10460–10473. https://doi.org/10.1128/JVI.00783-07.
60. Wang GG, Calvo KR, Pasillas MP, Sykes DB, Hacker H, Kamps MP. 2006. Quantitative production of macrophages or neutrophils ex vivo using conditional Hoxb8. Nat Methods 3:287–293. https://doi.org/10.1038/nmeth865.
61. Lazear HM, Nice TJ, Diamond MS. 2015. Interferon-lambda: immune functions at barrier surfaces and beyond. Immunity 43:15–28. https://doi.org/10.1016/j.immuni.2015.07.001.
62. Durbin RK, Kotenko SV, Durbin JE. 2013. Interferon induction and function at the mucosal surface. Immunol Rev 255:25–39. https://doi.org/10.1111/imr.12101.
63. Orchard RC, Wilen CB, Doench JG, Baldridge MT, McCune BT, Lee YC, Lee S, Pruett-Miller SM, Nelson CA, Fremont DH, Virgin HW. 2016. Discovery of a proteinaceous cellular receptor for a norovirus. Science 353:933–936. https://doi.org/10.1126/science.aaf1220.
64. Gitlin L, Barchet W, Gilfillan S, Cella M, Beutler B, Flavell RA, Diamond MS, Colonna M. 2006. Essential role of mda-5 in type I IFN responses to polyriboinosinic:polyribocytidylic acid and encephalomyocarditis picornavirus. Proc Natl Acad Sci U S A 103:8459–8464. https://doi.org/10.1073/pnas.0603082103.
65. Wilen CB, Lee S, Hsieh LL, Orchard RC, Desai C, Hykes BL, Jr, McAllaster MR, Balce DR, Feehley T, Brestoff JR, Hickey CA, Yokoyama CC, Wang YT, MacDuff DA, Kreamalmayer D, Howitt MR, Neil JA, Cadwell K, Allen PM, Handley SA, van Lookeren Campagne M, Baldridge MT, Virgin HW. 2018. Tropism for tuft cells determines immune promotion of norovirus pathogenesis. Science 360:204–208. https://doi.org/10.1126/science.aar3799.
66. Ward VK, McCormick CJ, Clarke IN, Salim O, Wobus CE, Thackray LB, Virgin HW, Lambden PR. 2007. Recovery of infectious murine norovirus using pol II-driven expression of full-length cDNA. Proc Natl Acad Sci U S A 104:11050–11055. https://doi.org/10.1073/pnas.0700336104.
67. Edelmann KH, Richardson-Burns S, Alexopoulou L, Tyler KL, Flavell RA, Oldstone MB. 2004. Does Toll-like receptor 3 play a biological role in virus infections? Virology 322:231–238. https://doi.org/10.1016/j.virol.2004.01.033.
68. Lopez CB, Moltedo B, Alexopoulou L, Bonifaz L, Flavell RA, Moran TM. 2004. TLR-independent induction of dendritic cell maturation and adaptive immunity by negative-strand RNA viruses. J Immunol 173:6882–6889. https://doi.org/10.4049/jimmunol.173.11.6882.
69. Liu S, Chen J, Cai X, Wu J, Chen X, Wu YT, Sun L, Chen ZJ. 2013. MAVS recruits multiple ubiquitin E3 ligases to activate antiviral signaling cascades. Elife 2:e00785. https://doi.org/10.7554/eLife.00785.
70. Loo YM, Fornek J, Crochet N, Bajwa G, Perwitasari O, Martinez-Sobrido L, Akira S, Gill MA, Garcia-Sastre A, Katze MG, Gale M, Jr. 2008. Distinct RIG-I and MDA5 signaling by RNA viruses in innate immunity. J Virol 82:335–345. https://doi.org/10.1128/JVI.01080-07.
71. Berke IC, Li Y, Modis Y. 2013. Structural basis of innate immune recognition of viral RNA. Cell Microbiol 15:386–394. https://doi.org/10.1111/cmi.12061.
72. Bruns AM, Horvath CM. 2014. Antiviral RNA recognition and assembly by RLR family innate immune sensors. Cytokine Growth Factor Rev 25:507–512. https://doi.org/10.1016/j.cytogfr.2014.07.006.
73. Sohn J, Hur S. 2016. Filament assemblies in foreign nucleic acid sensors. Curr Opin Struct Biol 37:134–144. https://doi.org/10.1016/j.sbi.2016.01.011.
74. Roth AN, Karst SM. 2016. Norovirus mechanisms of immune antagonism. Curr Opin Virol 16:24–30. https://doi.org/10.1016/j.coviro.2015.11.005.
75. Oshiumi H, Kouwaki T, Seya T. 2016. Accessory factors of cytoplasmic viral RNA sensors required for antiviral innate immune response. Front Immunol 7:200. https://doi.org/10.3389/fimmu.2016.00200.
76. Gack MU, Shin YC, Joo CH, Urano T, Liang C, Sun L, Takeuchi O, Akira S, Chen Z, Inoue S, Jung JU. 2007. TRIM25 RING-finger E3 ubiquitin ligase is essential for RIG-I-mediated antiviral activity. Nature 446:916–920. https://doi.org/10.1038/nature05732.
77. Strong DW, Thackray LB, Smith TJ, Virgin HW. 2012. Protruding domain of capsid protein is necessary and sufficient to determine murine norovirus replication and pathogenesis in vivo. J Virol 86:2950–2958. https://doi.org/10.1128/JVI.07038-11.
78. Whelan SP, Barr JN, Wertz GW. 2000. Identification of a minimal size requirement for termination of vesicular stomatitis virus mRNA: implications for the mechanism of transcription. J Virol 74:8268–8276. https://doi.org/10.1128/JVI.74.18.8268-8276.2000.
79. Durbin JE, Hackenmiller R, Simon MC, Levy DE. 1996. Targeted disruption of the mouse Stat1 gene results in compromised innate immunity to viral disease. Cell 84:443–450. https://doi.org/10.1016/S0092-8674(00)81289-1.
80. Wooten RM, Ma Y, Yoder RA, Brown JP, Weis JH, Zachary JF, Kirschning CJ, Weis JJ. 2002. Toll-like receptor 2 is required for innate, but not acquired, host defense to Borrelia burgdorferi. J Immunol 168:348–355. https://doi.org/10.4049/jimmunol.168.1.348.
81. Alexopoulou L, Holt AC, Medzhitov R, Flavell RA. 2001. Recognition of double-stranded RNA and activation of NF-kappaB by Toll-like receptor 3. Nature 413:732–738. https://doi.org/10.1038/35099560.
82. Lund JM, Alexopoulou L, Sato A, Karow M, Adams NC, Gale NW, Iwasaki A, Flavell RA. 2004. Recognition of single-stranded RNA viruses by Toll-like receptor 7. Proc Natl Acad Sci U S A 101:5598–5603. https://doi.org/10.1073/pnas.0400937101.
83. Hou B, Reizis B, DeFranco AL. 2008. Toll-like receptors activate innate and adaptive immunity by using dendritic cell-intrinsic and -extrinsic mechanisms. Immunity 29:272–282. https://doi.org/10.1016/j.immuni.2008.05.016.
84. Sun Q, Sun L, Liu HH, Chen X, Seth RB, Forman J, Chen ZJ. 2006. The specific and essential role of MAVS in antiviral innate immune responses. Immunity 24:633–642. https://doi.org/10.1016/j.immuni.2006.04.004.
85. Sato M, Suemori H, Hata N, Asagiri M, Ogasawara K, Nakao K, Nakaya T, Katsuki M, Noguchi S, Tanaka N, Taniguchi T. 2000. Distinct and essential roles of transcription factors IRF-3 and IRF-7 in response to viruses for IFN-alpha/beta gene induction. Immunity 13:539–548. https://doi.org/10.1016/S1074-7613(00)00053-4.
86. Honda K, Yanai H, Negishi H, Asagiri M, Sato M, Mizutani T, Shimada N, Ohba Y, Takaoka A, Yoshida N, Taniguchi T. 2005. IRF-7 is the master regulator of type-I interferon-dependent immune responses. Nature 434:772–777. https://doi.org/10.1038/nature03464.
87. Platt RJ, Chen S, Zhou Y, Yim MJ, Swiech L, Kempton HR, Dahlman JE, Parnas O, Eisenhaure TM, Jovanovic M, Graham DB, Jhunjhunwala S, Heidenreich M, Xavier RJ, Langer R, Anderson DG, Hacohen N, Regev A, Feng G, Sharp PA, Zhang F. 2014. CRISPR-Cas9 knockin mice for genome editing and cancer modeling. Cell 159:440–455. https://doi.org/10.1016/j.cell.2014.09.014.
88. Sanjana NE, Shalem O, Zhang F. 2014. Improved vectors and genome-wide libraries for CRISPR screening. Nat Methods 11:783–784. https://doi.org/10.1038/nmeth.3047.
89. Shalem O, Sanjana NE, Hartenian E, Shi X, Scott DA, Mikkelson T, Heckl D, Ebert BL, Root DE, Doench JG, Zhang F. 2014. Genome-scale CRISPR-Cas9 knockout screening in human cells. Science 343:84–87. https://doi.org/10.1126/science.1247005.
90. Baert L, Wobus CE, Van Coillie E, Thackray LB, Debevere J, Uyttendaele M. 2008. Detection of murine norovirus 1 by using plaque assay, transfection assay, and real-time reverse transcription-PCR before and after heat exposure. Appl Environ Microbiol 74:543–546. https://doi.org/10.1128/AEM.01039-07.